



A viscosity method for Shape-from-Shading without boundary data

Emmanuel Prados, Fabio Camilli, Olivier Faugeras

► To cite this version:

Emmanuel Prados, Fabio Camilli, Olivier Faugeras. A viscosity method for Shape-from-Shading without boundary data. RR-5296, INRIA. 2004, pp.35. inria-00070704

HAL Id: inria-00070704

<https://inria.hal.science/inria-00070704>

Submitted on 19 May 2006

HAL is a multi-disciplinary open access archive for the deposit and dissemination of scientific research documents, whether they are published or not. The documents may come from teaching and research institutions in France or abroad, or from public or private research centers.

L'archive ouverte pluridisciplinaire **HAL**, est destinée au dépôt et à la diffusion de documents scientifiques de niveau recherche, publiés ou non, émanant des établissements d'enseignement et de recherche français ou étrangers, des laboratoires publics ou privés.

A viscosity method for Shape-from-Shading without boundary data

Emmanuel Prados — Fabio Camilli — Olivier Faugeras

N° 5296

August 2004

_____ Thèmes COG et NUM _____



*rapport
de recherche*

A viscosity method for Shape-from-Shading without boundary data

Emmanuel Prados^{*}, Fabio Camilli[†], Olivier Faugeras[‡]

Thèmes COG et NUM — Systèmes cognitifs et Systèmes numériques
Projet Odysée

Rapport de recherche n° 5296 — August 2004 — 35 pages

Abstract: This report proposes a solution of the Lambertian Shape From Shading (SFS) problem by designing a *new mathematical framework* based on the notion of *viscosity solutions*. The power of our approach is twofolds: 1) it defines a notion of *weak* solutions (in the viscosity sense) which *does not necessarily require boundary data*. Note that, in the previous SFS work of Rouy et al. [45, 32], Falcone et al. [23, 22], Prados et al. [43, 41], the characterization of a viscosity solution and its computation require the knowledge of its values on the boundary of the image. This was quite unrealistic because in practice such values are not known. 2) it *unifies* the work of Rouy et al. [45, 32], Falcone et al. [22, 23], Prados et al. [43, 41], based on the notion of viscosity solutions and the work of Dupuis and Oliensis [20] dealing with classical (C^1) solutions and value functions. Also, we *generalize* their work to the “perspective SFS” problem recently introduced by Prados and Faugeras [41]. The notion of viscosity solutions described in this paper is obtained by slightly modifying the notion of singular viscosity solutions developed by Camilli and Siconolfi [11, 12]. We demonstrate the existence and the uniqueness of the solution for a class of Hamilton-Jacobi equations

$$H(x, \nabla u) = 0,$$

in a bounded open domain. Some stability results are proved. Moreover, we show that this framework allows to characterize the classical discontinuous viscosity solutions by their “minimum”.

In this report, we also propose some algorithms which provide numerical approximations of these new solutions. These provably convergent algorithms are quite *robust* and do not necessarily require boundary data. Finally, we have successfully applied our SFS method to real images and we have suggested a number of real-life applications.

Key-words: Shape from Shading, boundary data, unification of SFS theories, singular viscosity solutions, states constraints, Sonner’s boundary conditions.

^{*} <http://www-sop.inria.fr/odyssee/> (Odysée Lab., INRIA/ENS/ENPC, France)

[†] camilli@ing.univaq.it (Pure and Applied Mathematics Department of the University of L’Aquila, Italy)

[‡] <http://www-sop.inria.fr/odyssee/> (Odysée Lab., INRIA/ENS/ENPC, France)

Shape-from-Shading “sans” condition aux limites

Résumé : Ce rapport propose une solution au problème du “Shape-From-Shading” (SFS) Lambertien en construisant *un nouveau cadre mathématique* basé sur la notion de solutions de viscosité. Le pouvoir de notre approche est double: 1) il définit une notion de solutions *faibles* (dans le sens des solutions de viscosité) qui *ne nécessite pas forcément de données au bord* (contrairement aux notions utilisées dans [45, 32, 22, 23, 43, 41]). 2) il *unifie* les travaux de Rouy et al.[45, 32], Falcone et al. [22, 23], Prados et al. [43, 41], basés sur la notion de solutions de viscosité et les travaux de Dupuis et Oliensis [20] qui considèrent les solutions C^1 classiques et les fonctions valeurs. Nous *généralisons* aussi tous ces travaux au problème de “*SFS perspectif*” introduit récemment par Prados et Faugeras [41].

Dans ce rapport, nous proposons aussi des méthodes permettant d’approcher numériquement ces nouvelles solutions. Nous prouvons la convergence des approximations numériques calculées vers la solution de l’EDP. Nous démontrons l’applicabilité de nos algorithmes de SFS à des images réelles et nous suggérons des applications.

Mots-clés : “Shape from Shading”, solutions de viscosité singulières, contraintes d’états, conditions de Soner, unification des théories.

1 Introduction

The application of the theory of Partial Differential Equations (PDEs) to the Shape from Shading (SFS) problem has been hampered by several types of difficulties. The first type arises from the kind of modelling that is used: orthographic cameras looking at Lambertian objects with a single point light source at infinity is the set of usual assumptions [56, 27]. The second type is mathematical: characterizing the solution(s) of the corresponding PDE has turned out to be a very difficult problem; boundary conditions are assumed to be known, say at image boundary, in contradiction with real practice [45, 43, 10, 22, 23]. The third type is algorithmic: assuming that existence has been proved, coming up with provably convergent numerical schemes has turned out to be quite involved [21].

Our approach is therefore based upon the interaction of the following three ingredients:

1. Analytic: We use and adapt the notion of viscosity solutions to solve such basic problems as the existence and uniqueness of a solution or the characterization of all solutions when uniqueness does not hold.
2. Algorithmic: In [5], Barles and Souganidis propose a large class of approximation schemes (the so called monotonous) of viscosity solutions. Inspired by their work, we build such schemes for the SFS equations from which we obtain algorithms whose properties we can analyze in detail (stability, convergence, accuracy). This results in provably correct algorithms within a set of well-defined assumptions.
3. Modeling: The theory of viscosity solutions previously used in SFS area [45, 43, 41, 10, 22, 23] is not well-adapted to the natural constraints of the SFS problem. In particular it requires that boundary conditions be given, e.g. at the image boundary, and creates undesirable folds (see section 3). In order to be able to get rid of this constraint, we consider a “new” notion of viscosity solutions, by adapting the notion of singular viscosity solutions of Camilli and its coworkers [9, 11, 12].

Our contributions are first theoretic: we introduce a “new” class of viscosity solutions which is really more suitable to the SFS problem than the previous ones. This original mathematical framework is general and allows to improve and unify the work of [45, 43, 41, 10, 23, 20]. Directly connected to the area of modeling, thanks to the introduction of this framework, we are able to relax the very constraining assumption that boundary conditions are known. The second contribution of this report lies on a proof of the applicability of our SFS method to *real images* and on a suggestion of various applications in three different areas.

2 Hamiltonians for the Lambertian SFS problem

In this section, we recall various formulations of the SFS problem. We deal with Lambertian scenes and suppose that the albedo is constant and equal to 1. Let Ω be the image domain. We represent the scene by a surface \mathbf{S} which can be explicitly parameterized by using the function $S : \overline{\Omega} \rightarrow \mathbb{R}^3$:

$$\mathbf{S} = \{S(x); \quad x \in \overline{\Omega}\}.$$

2.1 “Orthographic SFS” with a point light source at infinity

This is the traditional setup for the SFS problem. We denote by $\mathbf{L} = (\alpha, \beta, \gamma)$ the unit vector representing the direction of the light source ($\gamma > 0$), $\mathbf{l} = (\alpha, \beta)$. The function S parameterizing the surface \mathbf{S} is given by $S(x) = (x, u(x))$. The SFS problem is then, given I and \mathbf{L} , to find a function $u : \overline{\Omega} \rightarrow \mathbb{R}$ satisfying the following brightness equation:

$$\forall x \in \Omega, \quad I(x) = (-\nabla u(x) \cdot \mathbf{l} + \gamma) / \sqrt{1 + |\nabla u(x)|^2},$$

This classical equation has been associated to various Hamiltonians:

- 1) In [45], Rouy and Tourin introduce

$$H_{R/T}^{orth}(x, p) = I(x) \sqrt{1 + |p|^2} + p \cdot \mathbf{l} - \gamma.$$

- 2) In [20], Dupuis and Oliensis consider

$$H_{D/O}^{orth}(x, p) = I(x) \sqrt{1 + |p|^2} - 2p \cdot \mathbf{l} + p \cdot \mathbf{l} - 1.$$

- 3) For $\mathbf{L} = (0, 0, 1)$, Lions et al. [32] deal with: $H_{Eko}^{orth}(x, p) = |p| - \sqrt{\frac{1}{I(x)^2} - 1}$ (eikonal equation).

2.2 “Perspective SFS” with a point light source at infinity

In [41], we parameterize the surface \mathbf{S} by defining $S(x) = u(x) (x, -f)$. Combining the expression of $\mathbf{n}(x)$ and the change of variables $v = \ln(u)$, we obtain from the irradiance equation the following Hamiltonian¹:

$$H_{P/F}^{pers}(x, p) = I(x) \sqrt{f^2 |p|^2 + (x \cdot p + 1)^2} - (f + \gamma x) \cdot p - \gamma.$$

See [40], for more details.

2.3 “Perspective SFS” with a point light located at the optical center

This model corresponds nicely to the situation encountered in some medical protocols like endoscopy or colposcopy, in which the (point) light source is located very close to the camera, because of space constraints, see section 8.3 for a SFS application in this area. This modeling also corresponds approximately to the situation encountered when we use a simple camera equipped with a flash; see sections 8.1 and 8.2 for two applications (face reconstruction and page restoration). In [40], we parameterize the surface \mathbf{S} by defining $S(x) = \frac{f \cdot u(x)}{\sqrt{|x|^2 + f^2}} (x, -f)$. Combining the expression of the normal vectors $\mathbf{n}(x)$, the expression of light source direction and the change of variables $v = \ln(u)$, we obtain from the irradiance equation the following Hamiltonian:

$$H_F^{pers}(x, p) = I(x) \sqrt{f^2 |p|^2 + (p \cdot x)^2 + Q(x)^2} - Q(x),$$

where $Q(x) = \sqrt{f^2 / (|x|^2 + f^2)}$. See [40], for more details.

2.4 A generic Hamiltonian

In [40], we prove that all the previous SFS Hamiltonians (H_F^{pers} , $H_{R/T}^{orth}$, $H_{D/O}^{orth}$, H_{Eiko}^{orth} , and $H_{P/F}^{pers}$) are special cases of the following “generic” Hamiltonian:

$$H_g(x, p) = \tilde{H}_g(x, A_x p + \vec{v}_x) + \vec{w}_x \cdot p + c_x,$$

with $\tilde{H}_g(x, q) = \kappa_x \sqrt{|q|^2 + K_x^2}$, $\kappa_x, K_x \geq 0$, $A_x = D_x R_x$, $D_x = \begin{pmatrix} \mu_x & 0 \\ 0 & \nu_x \end{pmatrix}$, R_x is the rotation matrix $\frac{1}{|x|} \begin{pmatrix} x_2 & -x_1 \\ x_1 & x_2 \end{pmatrix}$ if $x \neq 0$, $R_x = Id_2$ if $x = 0$, $\mu_x, \nu_x \in \mathbb{R}^*$ (i.e. $\mu_x, \nu_x \neq 0$), $\vec{v}_x, \vec{w}_x \in \mathbb{R}^2$ and $c_x \in \mathbb{R}$.

By using the Legendre transform, we rewrite this “generic” Hamiltonian as a supremum:

$$H_g(x, p) = \sup_{a \in B_2(0,1)} \{-f_g(x, a) \cdot p - l_g(x, a)\}.$$

In [40], we detail the exact expressions of f_g and l_g . This generic formulation considerably simplifies the analysis of the problem. In particular, this formulation *unifies the orthographic and perspective SFS problems*. Also, from a practical point of view, *a unique algorithm can be used to numerically solve these various problems*.

3 Weaknesses of the previous theoretical approaches of the SFS problem

The theory of viscosity solutions was first used to solve SFS problems by Lions, Rouy and Tourin [45, 32] in the 90s. Their work was based upon the notion of *continuous* viscosity solution. The viscosity solutions are PDE solutions in a weak sense. In particular, they are not necessarily differentiable and can have edges. Let us emphasize that continuous viscosity solutions are continuous (on the closure of the set where they are defined) and that a solution in the classical sense is a viscosity solution.

A drawback of this notion is due to the compatibility condition necessary to the existence of a solution (constraint on the variation of the boundary conditions [31]). For example, the equation

$$|\nabla u(x)| = 1 \text{ for all } x \text{ in }]0, 1[\tag{1}$$

with $u(0) = u(1) = 0$, does not have classical solutions but has a continuous viscosity solution (see figure 1-a)). The same equation (1) with $u(0) = 0$, $u(1) = 1.5$ does not have continuous viscosity solutions (see [40] for

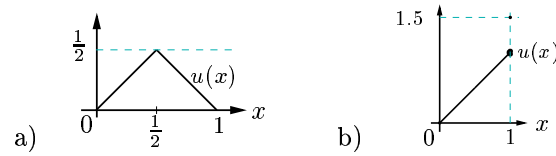


Figure 1: a) Continuous viscosity solution of (1) with $u(0) = u(1) = 0$; b) discontinuous viscosity solution of (1) with $u(0) = 0$ and $u(1) = 1.5$.

more details). Now let us suppose that we make a large error on the boundary condition, when we compute a numerical solution of the SFS problems. If this error is too large then there do not exist continuous viscosity solutions. In this case one may wonder what the numerical algorithm of [45, 32] computes. In [43], Prados et al. answer this question by proposing to use the more general idea of *discontinuous* viscosity solutions. For example, equation (1) with $u(0) = 0$, $u(1) = 1.5$ has a discontinuous viscosity solution (see figure 1-b) and see [44, 40] for more details). Let us emphasize that a “discontinuous viscosity solution” *can* have discontinuities and that a continuous viscosity solution is a discontinuous viscosity solution.

The classical theory of viscosity solutions offers simple and general theorems of existence and uniqueness of solutions for exactly the type of PDEs that arise in the context of SFS. In particular the theory allows to characterize exactly all possible continuous viscosity solutions: given a particular Dirichlet condition on the image boundary (verifying the compatibility condition), if the set of *critical points* (points of maximal intensity, i.e. $I(x) = 1$) is empty, then there exists a unique continuous viscosity solution satisfying the boundary conditions. If the set of critical points is not empty there exists an infinity of continuous viscosity solutions which are characterized by their values at the critical points. Note that this result is general and applies equally to all the SFS models described in section 2 (see [40]). As a consequence, the SFS problem is ill-posed and to compute a numerical approximation of a solution, Rouy et al. and Prados et al. [45, 43, 41] must assume that the values of the solutions are given at the image boundary and at the critical points. This is quite unsatisfactory, even more so since small errors on these values create undesirable crests, see figure 2-b) or [43] for an example with a real image.

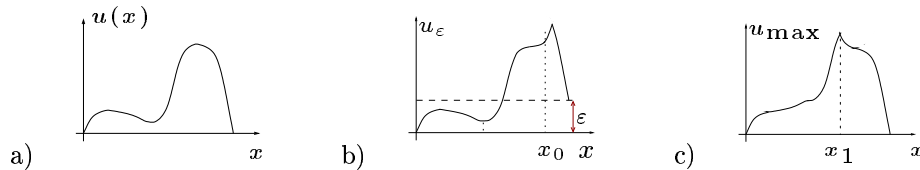


Figure 2: a) original surface u ; b) solution u_ε associated to corrupted boundary conditions and to the image obtained from the original surface a) with the Eikonal equation; c) maximal solution u_{\max} (in Falcone’s sense [10, 22, 23]) associated to the same image. u_ε and u_{\max} present a kink at x_0 and x_1 .

Falcone [10, 22, 23] proposes to not specify anymore the values of the solution at the critical points (he still requires to specify the values at the image boundary though). In order to achieve this, he uses the notion of “maximal” viscosity solutions developed by Camilli and Siconolfi [10, 11, 9]. Despite its advantages, this approach is not really adapted to the SFS problem, see for example figure 2-c). In this figure, the maximal solution u_{\max} associated to the image obtained from the original surface u shows a highly visible crest where the surface should be smooth. Even with the correct boundary conditions, Falcone’s method does not allow to recover the original surface, but only the maximal surface with the same brightness $I(x)$.

To summarize the work of Rouy et al. [45], Prados et al. [43, 41] and Falcone et al. [10, 22, 23] suggests theories and numerical methods based on the concept of viscosity solutions and requiring data on the boundary of the image. At the opposite, Dupuis and Oliensis [20] consider C^1 solutions. They characterize a C^1 solution by specifying only its values at the critical points which are local minima. In particular, they do not specify the values of the solution on the boundary of the image. Also, they provide algorithms for approximating these smooth solutions. Nevertheless, in practice, because of noise, of incorrect modeling, errors on parameters or on the depth values enforced at the critical points, there do not exist C^1 solutions to the SFS equations [36].

Considering the drawbacks and the advantages of all these methods, it seems important to consider an other class of weak solutions such that the characterization of Dupuis and Oliensis holds, and which provides a (theoretical

¹ This Hamiltonian was first introduced in [39]

and numerical) solution when there do not exist smooth solutions.

As we show in the second part of section 3.5.3 of [40], the notion of discontinuous viscosity solutions does not allow to impose the values of the solution at the critical points (this does not allow to characterize the discontinuous viscosity solutions). Therefore, this notion cannot provide an extension of the Dupuis and Oliensis work. On the other side, the notion of singular viscosity solutions developed by Camilli and Siconolfi in [11, 9, 12] uses Dirichlet conditions all around the boundary of the image. Thus, it does not also provide a direct extension of the Dupuis and Oliensis work.

For such an extension, we must slightly modify these notions and we must consider a “new” type of boundary conditions (called “state constraints” [48]). It turns out that the correct notion of viscosity solution for the SFS problem is the “singular discontinuous viscosity solution with Dirichlet boundary conditions and state constraints”. These solutions can be interpreted as maximal solutions and have the great advantage of not necessarily requiring boundary or critical points conditions. Moreover, this notion provides a mathematical framework unifying the work of Rouy et al. [32, 45], Prados et al. [43, 41], Falcone et al. [10, 22, 23] and Dupuis and Oliensis [20].

4 Singular discontinuous viscosity solutions with Dirichlet boundary conditions and state constraints (SDVS)

The notion of singular viscosity solutions was pioneered by Ishii and Ramaswamy [28] and has been recently upgraded by Camilli and Siconolfi [11, 9, 12]. In this section, we slightly modify the tools developed in these papers introducing the notion of “singular viscosity solution with Dirichlet boundary conditions and state constraints” (SDVS), and we prove the existence and uniqueness of the SDVS for the Shape from Shading problems.

Let Ω be a bounded open subset of \mathbb{R}^N with smooth boundary (say $W^{2,\infty}$). In the SFS problem $N = 2$. So Ω is a smooth part of rectangular domain $]0, X[\times]0, Y[$ which typically represents the domain of definition of the image. We consider the partial differential equation (PDE):

$$H(x, \nabla u) = 0, \quad \forall x \in \Omega, \quad (2)$$

where $H : \overline{\Omega} \times \mathbb{R}^N \rightarrow \mathbb{R}$ is a continuous, *convex* (with respect to p) Hamiltonian, and satisfies the coercitivity condition

$$\liminf_{|p| \rightarrow +\infty} H(x, p) = +\infty, \quad \text{for any } x \in \overline{\Omega}. \quad (3)$$

Moreover we assume that there exists a subsolution $\psi \in C^1(\Omega) \cap W^{1,\infty}(\Omega)$ of (2) (i.e: $\forall x \in \Omega, H(x, \nabla \psi(x)) \leq 0$) and

$$\begin{aligned} &\text{for any } \lambda \in (0, 1), p \in \mathbb{R}^N \text{ s.t. } H(x, p) \leq 0 \text{ then} \\ &H(x, \lambda p + (1 - \lambda) \nabla \psi(x)) < 0. \end{aligned} \quad (4)$$

Note that the previous hypotheses hold for all the SFS Hamiltonians considered in Section 2 (see [40]) as soon as the intensity image I is continuous and verifies $I(x) > 0$ for any $x \in \overline{\Omega}$.

We say that ψ is a strict subsolution of (2) at x when $H(x, \nabla \psi(x)) < 0$. We denote by \mathcal{S} the set of *singular points* of H respect to ψ :

$$\mathcal{S} = \{x \in \overline{\Omega} \mid H(x, \nabla \psi(x)) = 0\},$$

i.e. the set where ψ fails to be a strict subsolution of (2). \mathcal{S} is closed by the continuity of $\nabla \psi$ and H .

We also assume that

$$\mathcal{S} \cap \partial\Omega = \emptyset. \quad (5)$$

We recall that if \mathcal{S} is empty then there exists a unique viscosity solution to (2) completed with an appropriate boundary condition. If \mathcal{S} is not empty, then in general uniqueness fails.

REMARKS 1.

R1.1 - In the case where H is an Hamilton-Jacobi-Bellman (HJB) Hamiltonian

$$H(x, p) = \sup_{a \in A} \{-f(x, a) \cdot p - l(x, a)\} \quad (6)$$

with $f : \overline{\Omega} \times A \rightarrow \mathbb{R}^N$, $l : \overline{\Omega} \times A \rightarrow \mathbb{R}$ and the “cost” l is nonnegative, \mathcal{S} corresponds to the set

$$\{x \in \overline{\Omega} \mid l(x, a) = 0 \text{ for some } a \in A\}.$$

In this case $\psi \equiv 0$ is a subsolution of the equation. Yet, at the opposite to [9], in this paper we do not assume that l is a nonnegative function. As it was shown in [40] (see Section 3.5), the Rouy/Tourin Hamiltonian $H_{R/T}^{orth}$ (where, $l_{R/T}(x, a) = I(x)\sqrt{1 + |a|^2} - \gamma$) and the perspective Hamiltonian $H_{P/F}^{pers}$, which fit in the class of Hamiltonians given by (6) but with a cost of arbitrary sign, admit a regular subsolution. Therefore, in this report, to each SFS Hamiltonian we systematically associate the corresponding subsolution ψ defined in [40].

R1.2 - In [40], Section 3.5, we prove that for all the SFS equations presented in Section 2 the set of singular points \mathcal{S} corresponds to the set of “critical points” $\{x \in \overline{\Omega} \mid I(x) = 1\}$ where I is the intensity image. Note that in the SFS problem, even if we do not make this assumption, it may appear natural to assume that $\mathcal{S} = \{x_1, \dots, x_k\}$, since the situation where $\overset{\circ}{\mathcal{S}}$ (the interior of the set \mathcal{S}) is not empty, is non generic². Nevertheless, in practice, due to some saturation or discretisation effects, several connected points can have an intensity equal to the maximal intensity (i.e $I(x) = 1$).

R1.3 - As we have shown in Section 3.4.1 of [40], the coercivity hypothesis (3) is not systematically verified for all the SFS Hamiltonians. Globally, it does not hold for the pixels of the image with a low brightness, i.e. $I(x)$ close to 0, when the direction of the distant light source is very different to the one of the camera. In this work, we do not weaken this hypothesis explaining in various remarks some difficulties involved by the non coercivity.

Definition 1 *Let u be a locally bounded function on a set E .*

For any $x \in E$, we set:

$$\begin{aligned} u^*(x) &= \limsup_{y \rightarrow x} u(y) = \sup \{ \limsup_{n \rightarrow \infty} u(x_n) : x_n \rightarrow x \}, \\ u_*(x) &= \liminf_{y \rightarrow x} u(y) = \inf \{ \liminf_{n \rightarrow \infty} u(x_n) : x_n \rightarrow x \}. \end{aligned}$$

u^* and u_* are respectively called the upper semicontinuous envelope and lower semicontinuous envelope of u .

Recall that, if u is a locally bounded function, then u^* is u.s.c and u_* is l.s.c. (see sections V-1 and V-2.1 of [1] for more details).

We now give the definition of viscosity subsolution. The definition of viscosity supersolution, which is modified respect to the standard one to solve the uniqueness issue, is postponed to the next subsection.

Definition 2 (Viscosity subsolution of (2)) *A locally bounded function u , u.s.c in Ω , is said a viscosity subsolution of equation (2) if*

$$\forall \phi \in C^1(\Omega), \forall x_0 \in \Omega \quad \text{local maximum of } (u - \phi), \quad H(x_0, \nabla \phi(x_0)) \leq 0.$$

The regularity of $\partial\Omega$ and the hypothesis on H imply that a viscosity subsolution of (2) is Lipschitz continuous in Ω and moreover (see Prop. 4.3 in [11])

Proposition 1 *The following three properties are equivalent*

- u is a viscosity subsolution of (2) in Ω ;
- u is a Lipschitz continuous a.e. subsolution of (2) in Ω ;
- u is Lipschitz continuous and, defined the (Clarke) generalized gradient [17] by

$$\partial u(x) = \overline{\text{co}}\{p \in \mathbb{R}^N : p = \lim_{n \rightarrow \infty} \nabla u(x_n) \text{ for a sequence } x_n \in \text{Dom}(\nabla u) \text{ converging to } x\},$$

then the inequality

$$H(x, p) \leq 0$$

holds for any $x \in \Omega$, $p \in \partial u(x)$.

² In effect, for a given experimental setup (surface, light, camera) such that $\overset{\circ}{\mathcal{S}} \neq \emptyset$, an arbitrarily small change in the experimental parameters (for example, when the light moves) will make $\overset{\circ}{\mathcal{S}} = \emptyset$. An image such that $\overset{\circ}{\mathcal{S}} \neq \emptyset$ is highly unlikely.

REMARK 2. If the Hamiltonian is noncoercive then the subsolutions are not necessarily Lipschitz continuous. Moreover, subsolutions can yield discontinuities at the points x where $p \mapsto H(x, p)$ is non coercive. Nevertheless, note that, if \mathcal{S} is empty, only the coercivity on a *neighborhood* of $\partial\Omega$ is sufficient for ensuring the strong uniqueness, and so the continuity of the discontinuous viscosity solution on Ω . For a proof of this fact, see for example Theorem 4.5 of [3] and more especially its Corollary 4.1. In this corollary, the "HNCL" hypotheses of [3] is implied by convexity, existence of a strict subsolution and regularity of the Hamiltonian. The coercivity hypotheses (H18) and (H20) of [3] are only required on a neighborhood of $\partial\Omega$. The reader can also refer to [4].

With equation (2), we associate the Dirichlet boundary conditions (DBC)

$$u(x) = \varphi(x), \quad \forall x \in \partial\Omega \cup \mathcal{S} \quad (7)$$

where φ is defined on $\partial\Omega \cup \mathcal{S}$ into $\mathbb{R} \cup \{+\infty\}$, l.s.c., bounded from below and continuous in $\{x \in \partial\Omega \cup \mathcal{S} : \varphi(x) < +\infty\}$, with $\varphi \not\equiv +\infty$. At points x where $\varphi(x) = +\infty$, we say that we impose a *state constraint* boundary condition (see [48], [14]).

Definition 3 (Viscosity subsolution of (2)-(7)) *A locally bounded function u , u.s.c on $\overline{\Omega}$, is said a viscosity subsolution of (2)-(7) if u is a viscosity subsolution of (2) and if:*

- $\forall x_0 \in \mathcal{S}, \quad u(x_0) \leq \varphi(x_0).$
- $\forall x_0 \in \partial\Omega,$
 - $u(x_0) \leq \varphi(x_0)$
 - or $\forall \phi \in C^1(\overline{\Omega})$ s.t. x_0 is a local maximum of $(u - \phi)$, $H(x_0, \nabla \phi(x_0)) \leq 0$.

Note that points $x \in \partial\Omega$ where $\varphi(x) = +\infty$, the boundary condition is automatically satisfied.

4.1 Singular viscosity supersolutions of (2)-(7)

Before giving the definition of the singular viscosity supersolution of (2)-(7), we need to detail various assumptions and definitions.

4.1.1 The multivalued map

Let $\mathcal{Z}(x)$ be the multivalued map on Ω defined as:

$$\mathcal{Z}(x) = \{p \in \mathbb{R}^N : H(x, p) \leq 0\}. \quad (8)$$

For all the SFS Hamiltonians considered in this paper, it is easy to see that:

$$\forall x \in \mathcal{S}, \quad \mathcal{Z}(x) = \{\nabla \psi(x)\}. \quad (9)$$

Therefore, in the sequel, we assume that hypothesis (9) holds.

REMARKS 3.

R3.1 - Under the hypothesis (9), the continuity of H provides a new characterization of \mathcal{S} :

$$x \in \mathcal{S} \iff \mathcal{Z}(x) = \{\nabla \psi(x)\}.$$

R3.2 - Assumption (9) and Proposition 1 imply that for a subsolution u , $\partial u(x) = \{\nabla \psi(x)\}$ for $x \in \mathcal{S}$. Therefore a subsolution u is strictly differentiable (see [17]) on the singular set.

By (3) and (4), the set-valued map $\mathcal{Z}(x)$ is continuous in $\overline{\Omega}$ respect to the Hausdorff metric. Moreover, for any $x \in \overline{\Omega}$, the set $\mathcal{Z}(x)$ is compact, convex and strictly star-shaped respect to $\nabla\psi(x)$ and

$$\partial\mathcal{Z}(x) = \{p \in \mathbb{R}^N \mid H(x, p) = 0\}. \quad (10)$$

As explained in [12], (10) is a geometric property which allows us to study the equation $H(x, \nabla u) = 0$ through the level sets $\mathcal{Z}(x)$. Let W an open subset of Ω . If $F(x, p)$ is any continuous function representing $\mathcal{Z}(x)$ in the sense that for all $x \in W$,

$$\begin{aligned} F(x, p) &< 0 \quad \text{if and only if} \quad p \in \overset{\circ}{\mathcal{Z}}(x), \\ F(x, p) &= 0 \quad \text{if and only if} \quad p \in \partial\mathcal{Z}(x), \end{aligned}$$

then the equation

$$F(x, \nabla u) = 0, \quad \forall x \in W$$

is equivalent to $H(x, \nabla u) = 0$ in W from a viscosity point of view. Moreover the definition of subsolution could be equivalently expressed by the condition $\nabla u(x) \in \mathcal{Z}(x)$ in viscosity sense for any $x \in \Omega$.

4.1.2 A new Hamiltonian with the same multivalued map

Now, let us introduce the gauge function $\rho(x, p)$ of $\mathcal{Z}(x)$. We set for any $x \in \overline{\Omega}$, $p \in \mathbb{R}^N$,

$$\rho(x, p) = \inf\{\lambda > 0 : \lambda^{-1}p + (1 - \lambda^{-1})\nabla\psi(x) \in \mathcal{Z}(x)\}. \quad (11)$$

As in [3, 2], (see also Proposition 5.1 of [12]), we can prove that the function ρ is l.s.c in $\overline{\Omega} \times \mathbb{R}^N$ (continuous in $(\overline{\Omega} \setminus \mathcal{S}) \times \mathbb{R}^N$) and verifies the homogeneity condition:

$$\forall \mu > 0 \quad \text{and} \quad \forall (x, p) \in \overline{\Omega} \times \mathbb{R}^N, \quad \rho(x, \mu p + (1 - \mu)\nabla\psi(x)) = \mu\rho(x, p). \quad (12)$$

Moreover, $p \in \mathcal{Z}(x)$ if and only if $\rho(x, p) \leq 1$. If $x \in \mathcal{S}$, we have $\rho(x, \nabla\psi(x)) = 0$ and $\rho(x, p)$ is infinite for $p \neq \nabla\psi(x)$. Then the equation

$$\rho(x, \nabla u) = 1, \quad \forall x \in \Omega$$

defines an equation equivalent to (2) in $\Omega \setminus \mathcal{S}$ and singular for $x \in \mathcal{S}$.

4.1.3 Adaptation of the topology

Now, let us set, $\forall x \in \overline{\Omega}$,

$$r(x) = \sup\{r > 0 \mid B(\nabla\psi(x), r) \subset \mathcal{Z}(x)\}.$$

In [12], Lemma 3.1 it is proved that $r(x)$ is continuous in $\overline{\Omega}$, $r(x)$ is nonnegative and $r(x) = 0$ if and only if $x \in \mathcal{S}$.

REMARK 4. For the SFS Hamiltonians $H_{R/T}^{orth}, H_{D/O}^{orth}, H_{Eiko}^{orth}, H_F^{pers}$, it is possible to prove that $\forall x \in \overline{\Omega}$, $r(x)$ is finite and that $r(\cdot)$ is bounded on $\overline{\Omega}$ (even when these Hamiltonians are not coercive)³. The proof of Lemma 3.1 of [12] is essentially based on the fact that $r(\cdot)$ is bounded. Thus, this result applies to the previous SFS Hamiltonians, even at the points x where they are not coercive.

Note that by definition of $r(\cdot)$ and (9) we have

- $x \in \mathcal{S} \iff \mathcal{Z}(x) = \{\nabla\psi(x)\} \iff r(x) = 0$,
- $x \notin \mathcal{S} \iff \exists r > 0 \text{ s.t. } B(\nabla\psi(x), r) \subset \mathcal{Z}(x) \iff r(x) > 0$.

³ For the coercitivity of H_{Eiko}^{orth} and H_F^{pers} , we must assume that $I > 0$ on the compact set $\overline{\Omega}$.

As in [11, 12], we proceed defining a semidistance on $\overline{\Omega}$. We set for any $x, y \in \overline{\Omega}$,

$$S(x, y) = \inf \left\{ \int_0^1 r(\xi(t)) |\xi'(t)| dt : \xi(t) \in W^{1,\infty}([0, 1], \overline{\Omega}) \text{ s.t. } \xi(0) = x \text{ and } \xi(1) = y \right\}. \quad (13)$$

It is easy to verify that S satisfies:

$$S(x, y) \leq S(x, z) + S(z, y) \quad x, y, z \in \overline{\Omega},$$

$$S(x, y) = S(y, x) \quad x, y \in \overline{\Omega},$$

$$S(x, x) = 0 \quad x \in \overline{\Omega}$$

and

$$0 \leq S(x, y) \leq \|r\|_{\infty} d_E(x, y) \quad x, y \in \overline{\Omega}$$

where $d_E(x, y)$ is the Euclidean geodesic distance in Ω (i.e. the distance defined as in (13) with $r(x) \equiv 1$).

So S is a semidistance on $\overline{\Omega}$, but in general not a distance since, if $x_0 \in S$, the set of points which have 0 S -distance from x_0 is in general a subset of S containing elements different from x_0 . The family of balls:

$$B_S(x_0, R) = \{x \in \Omega \mid S(x_0, x) \leq R\}$$

induces a topology τ_S in Ω . Note that on a neighborhood of a point $x \in \Omega \setminus S$ the topology τ_S is equivalent to the Euclidean topology. At a point $x \in S$, it is a weaker topology.

We denote by $B_S(x_0)$ the subset

$$B_S(x_0) = \{x \in \overline{\Omega} \mid S(x_0, x) = 0\}.$$

4.1.4 Definition of singular viscosity supersolutions and solutions

Definition 4 (Strict subsolution of (2)) A function v is said to be a strict subsolution of (2) in an open subset A of Ω if v is a viscosity subsolution of

$$\rho(x, \nabla v) \leq \theta \quad x \in A$$

for some $\theta \in]0, 1[$.

Definition 5 ((Strict) Subtangent) For a l.s.c. function v , a Lipschitz continuous function ϕ is called S -subtangent to v at $x_0 \in \Omega$ if x_0 is a minimizer of $v - \phi$ in a τ_S -neighborhood of x_0 (or equivalently, in a neighborhood A of $B_S(x_0)$). The S -subtangent is called strict if the inequality

$$(v - \phi)(x) > (v - \phi)(x_0)$$

holds for $x \in A \setminus B_S(x_0)$.

Definition 6 (Singular viscosity supersolution of (2) at $x_0 \in \Omega$) A l.s.c. function $v : \Omega \rightarrow \mathbb{R}$ is said singular viscosity supersolution of (2) at $x_0 \in \Omega$, if it does not admit a S -subtangent at x_0 which is a strict subsolution of (2) in a neighborhood of $B_S(x_0)$.

Note: It is worth noting that if $x_0 \notin S$, the previous definition coincides with the standard notion of discontinuous viscosity supersolution of equation (2). We recall that that a locally bounded function v , l.s.c in Ω , is said a viscosity supersolution if

$$\forall \phi \in C^1(\Omega), \forall x_0 \in \Omega \quad \text{local minimum of } (u - \phi), \quad H(x_0, \nabla \phi(x_0)) \geq 0.$$

Definition 7 (Singular viscosity supersolution of (2)-(7)) A locally bounded function $v : \overline{\Omega} \rightarrow \mathbb{R}$, l.s.c. on $\overline{\Omega}$, is said singular viscosity supersolution of (2)-(7) if:

- $\forall x_0 \in \Omega \setminus S$, v is a singular viscosity supersolution of (2) at x_0 .
- $\forall x_0 \in \partial\Omega \cup S$,

- v is a singular viscosity supersolution of (2) at x_0
- or there exists $x \in B_S(x_0)$ such that $v(x_0) \geq \varphi(x) + \psi(x_0) - \psi(x)$.

Let us emphasize that, if the set of singular points \mathcal{S} is empty, then the singular supersolutions of (2)-(7) coincide with the standard discontinuous viscosity supersolutions of (2)-(7). Let us also recall that, at the points x_0 where $\varphi(x_0) = +\infty$, the Dirichlet boundary condition corresponds to a state constraint condition [48, 14].

Note that if $x_0 \in \mathcal{S}$, then $B_S(x_0)$ can be larger than $\{x_0\}$. As the definition of supersolution, also the boundary condition on \mathcal{S} is adapted to the weak topology induced by the semidistance S .

Now, we can give the definition of the singular viscosity solution of (2)-(7).

Definition 8 (Singular viscosity solution of (2)-(7))

A locally bounded function $u : \overline{\Omega} \rightarrow \mathbb{R}$ is said singular viscosity solution of (2)-(7) if u^* is a subsolution of (2)-(7) and if u_* is a singular supersolution of (2)-(7).

We will call “singular discontinuous viscosity solutions with Dirichlet boundary conditions and state constraints” (SDVS), the singular solution of (2)-(7).

4.2 Existence of the singular solution of (2)-(7)

In this section, we prove the existence of SDVS by giving an explicit representation formula of it.

Let $\delta : \Omega \times \mathbb{R}^N \rightarrow \mathbb{R}$ be the support function of the set $\tilde{\mathcal{Z}}(x) = \mathcal{Z}(x) \setminus \nabla\psi(x)$, i.e.:

$$\delta(x, p) = \max\{pq : q \in \tilde{\mathcal{Z}}(x)\}. \quad (14)$$

$\delta(x, p)$ is continuous in $\Omega \times \mathbb{R}^N$, convex and positively homogeneous in p and there exists R such that

$$0 \leq \delta(x, p) \leq R|p| \quad \forall x \in \overline{\Omega}, p \in \mathbb{R}^N \quad (15)$$

(see [12]).

For $A \subset \overline{\Omega}$, we denote: $\forall x, y \in \overline{A}$,

$$L_A(x, y) = \inf \left\{ \int_0^1 \delta(\xi(t), -\xi'(t)) dt \mid \xi(t) \in W^{1,\infty}([0, 1], \overline{A}) \text{ s.t. } \xi(0) = x \text{ and } \xi(1) = y \right\}$$

and we set $L(x, y) := L_\Omega(x, y)$. From (15) it follows that $0 \leq L(x, y) \leq R d_E(x, y)$ and therefore $y \mapsto L(x, y)$ is Lipschitz continuous in $\overline{\Omega}$ for any fixed $x \in \overline{\Omega}$ (with a Lipschitz constant which does not depend with respect to x).

REMARK 5. If $x \in \mathcal{S}$, then $\tilde{\mathcal{Z}}(x) = \{0\}$ and therefore $\delta(x, p) = 0$ for any $p \in \mathbb{R}^N$. Also, the inverse statement holds. Hence

$$\delta(x, p) = 0, \forall p \in \mathbb{R}^N \iff x \in \mathcal{S} \iff r(x) = 0.$$

So $\forall x, y \in \overline{\Omega}$,

$$L(x, y) = 0 \iff S(x, y) = 0.$$

In other words,

$$\forall x_0 \in \overline{\Omega}, \quad B_S(x_0) = \{x \in \Omega : L(x_0, x) = 0\}. \quad (16)$$

REMARK 6. When the Hamiltonian is not coercive, there can exist $x \in \overline{\Omega}$ such that $\mathcal{Z}(x)$ is unbounded. Hence for some $p \in \mathbb{R}^N$, we can have $\rho(x, p) = 0$ and $\delta(x, p) = +\infty$. So, for some $(x, y) \in \overline{\Omega} \times \overline{\Omega}$, we can have $L(x, y) = +\infty$. Note that, since L is in general nonsymmetric, it can result $L(y, x) < +\infty$.

Let us consider the function V :

$$V(x) = \psi(x) + \min\{ L(x, y) + \varphi(y) - \psi(y) \mid y \in \partial\Omega \cup \mathcal{S} \}. \quad (17)$$

Theorem 1 *The function V is a singular solution of (2)-(7).*

It is standard to prove that V is a viscosity subsolution of (2) (see [31, 14]). To show that V is a singular supersolution of (2)-(7), we need some preliminary results.

Proposition 2 *u is a subsolution of (2) in Ω if and only if*

$$u(x) \leq \psi(x) + u(y) - \psi(y) + L(x, y) \quad \text{for any } x, y \in \Omega \quad (18)$$

PROOF. See proposition 4.7 in [13]. □

Proposition 3 *Set*

$$\Gamma_V = \{x \in \mathcal{S} \mid V(x) \geq \varphi(y) + \psi(x) - \psi(y) \text{ for some } y \in B_S(x)\}.$$

If $x_0 \in \Omega \setminus \Gamma_V$, then $B_S(x_0) \cap \Gamma_V = \emptyset$.

PROOF. Assume by contradiction that there exists $x_1 \in B_S(x_0) \cap \Gamma_V$. Hence there exists $y \in B_S(x_1)$ such that $V(x_1) \geq \varphi(y) + \psi(x_1) - \psi(y)$. Since $S(x_0, y) \leq S(x_0, x_1) + S(x_1, y) = 0$, $y \in B_S(x_0)$. By (16), (18) and $x_0 \notin \Gamma_V$ we have

$$V(x_1) \leq V(x_0) + \psi(x_1) - \psi(x_0) < \varphi(y) + \psi(x_0) - \psi(y) + \psi(x_1) - \psi(x_0)$$

and so

$$V(x_1) < \varphi(y) + \psi(x_1) - \psi(y)$$

hence a contradiction. □

Proposition 4 (Dynamic programming principle) *For all $x \in \Omega \setminus \Gamma_V$ and all τ_S -neighborhood A of x s.t. $A \cap (\Gamma_V \cup \partial\Omega) = \emptyset$,*

$$V(x) = \psi(x) + \min_{y \in \partial A} \{L(x, y) + V(y) - \psi(y)\}. \quad (19)$$

PROOF. Classic; see for example [1]. □

Proposition 5 *Let u be a l.s.c. function, ϕ_0 a S -subtangent to u at a point x_0 and a strict subsolution of (2) in a τ_S -neighborhood of x_0 . Then there exists a function ϕ which is strict S -subtangent to u at x_0 and a strict subsolution of (2) in a τ_S -neighborhood of x_0 and such that for any $x \in \Omega$, $q \in \partial\phi(x)$, one can select $p \in \partial\phi_0(x)$ verifying*

$$\rho(x, q) \leq \rho(x, p) + L(x_0, x) \quad (20)$$

PROOF. See the proofs of Proposition 6.1 of [12] and of Proposition 5.1 of [11]. □

PROOF OF THEOREM 1. We argue by contradiction.

1. Let $x_0 \in \Omega \setminus \Gamma_V$. Let us assume that there exists a function ϕ_0 , a neighborhood A of $B_S(x_0)$ and $\theta \in]0, 1[$ s.t. ϕ_0 is a S -subtangent to V at x_0 with $\phi_0(x_0) = V(x_0)$ and

$$\rho(x, \nabla \phi_0) \leq \theta, \quad x \in A \quad (21)$$

in the viscosity sense.

Let ϕ be a strict S -subtangent to V at x_0 verifying the statement of Proposition 5. By continuity of the function $x \mapsto L(x_0, x)$ and (16), we can select a neighborhood A' of $B_S(x_0)$ and with $\overline{A'} \subset A$ satisfying

$$\sup_{x \in A'} L(x_0, x) < 1 - \theta, \quad (22)$$

$$\phi < V \quad \text{on} \quad \partial A' \quad (23)$$

and

$$A' \cap (\Gamma_V \cup \partial\Omega) = \emptyset. \quad (24)$$

Since $x_0 \in \Omega \setminus \Gamma_V$, we can assume the dynamic programming principle (19) holds on A' , so there exists $y_0 \in \partial A'$ such that

$$V(x_0) = \psi(x_0) + L_{A'}(x_0, y_0) + V(y_0) - \psi(y_0).$$

By

$$V(x_0) = \phi(x_0) \quad \text{and} \quad V(y_0) > \phi(y_0)$$

we get

$$L_{A'}(x_0, y_0) + [\phi(y_0) - \psi(y_0)] - [\phi(x_0) - \psi(x_0)] < 0.$$

So we can select a path $\xi \in W^{1,\infty}([0, 1], \overline{A'})$ joining x_0 to y_0 satisfying

$$\int_0^1 \left[\delta(\xi(t), -\dot{\xi}(t)) + \frac{d}{dt}(\phi(\xi(t)) - \psi(\xi(t))) \right] dt < 0.$$

Hence there exists $t_0 \in [0, 1]$ such that the functions $\phi(\xi(t))$ and $\xi(t)$ are differentiable at t_0 and

$$\delta(\xi(t_0), -\dot{\xi}(t_0)) - \dot{\xi}(t_0) \nabla \psi(\xi(t_0)) + \frac{d}{dt} \phi(\xi(t_0)) < 0. \quad (25)$$

Using the chain rule for the generalized gradient (see [17]), we derive from (25)

$$\delta(\xi(t_0), -\dot{\xi}(t_0)) < -\dot{\xi}(t_0)(q_0 - \nabla \psi(\xi(t_0)))$$

for some $q_0 \in \partial \phi(\xi(t_0))$. Hence

$$\rho(\xi(t_0), q_0) > 1.$$

Therefore by (20) and (22) the inequality

$$\rho(\xi(t_0), p_0) > \theta$$

holds for a suitable $p_0 \in \partial \phi_0(\xi(t_0))$. This contradicts (21) and Proposition 1 .

2. Let $x_0 \in \Gamma_V$. By definition of Γ_V , we have $V(x_0) \geq \varphi(x) + \psi(x_0) - \psi(x)$ for some $x \in B_S(x_0)$.
3. If $x_0 \in \partial\Omega$, assumption (5) implies that $B_S(x_0) = \{x_0\}$. If $V(x_0) > \varphi(x_0)$, assuming that the condition of viscosity supersolution does not hold, we can obtain a contradiction by adapting the proof of theorem V.4.13 of [1].

□

REMARKS 7.

r7.1 - Γ_V is the set where V takes the boundary datum φ in the sense of the topology τ_S .

R7.2 - In the case where the Hamiltonian is not coercive, we can have $V(x) = +\infty$, for some x in $\overline{\Omega}$. Nevertheless, note that this difficulty is mainly due to the state constraints. In effect if we assume that there exists $p_0 \in \mathbb{R}^N$ such that $\forall x \in \overline{\Omega}$, $\delta(x, p_0) \leq R < +\infty$ for some R not depending on x (this hypothesis holds for all the SFS Hamiltonians described in section 2) and if we enforce Dirichlet boundary conditions on $\partial\Omega$ (with Ω bounded), therefore

$$\forall x \in \overline{\Omega}, \quad V(x) < +\infty.$$

4.3 Uniqueness results

In this section we prove the uniqueness of the SDVS. This result applies for all the Shape from Shading equations described in section 2. We start this section with a maximum principle:

Theorem 2 (Maximum principle) *Let $u, v : \Omega \rightarrow \mathbb{R}$ be respectively an u.s.c. subsolution of (2) and a l.s.c. singular supersolution of (2)-(7). Let us denote*

$$\Gamma_v = \{x \in \mathcal{S} \mid v(x) \geq \varphi(y) + \psi(x) - \psi(y) \text{ for some } y \in B_S(x)\}.$$

Then

$$\min_{\overline{\Omega}} \{v - u\} = \min_{\partial\Omega \cup \Gamma_v} \{v - u\}.$$

PROOF. Given $\theta \in]0, 1[$, the function $u_\theta = \theta u + (1 - \theta)\psi(x)$ is a strict subsolution of (2) in Ω by the homogeneity of ρ (see (12)). Let us assume that $x_0 \in \Omega \setminus \Gamma_v$ is a minimizer of $(v - u_\theta)$ in $\overline{\Omega}$. Therefore u_θ is a S -subtangent of v at x_0 which is also a strict subsolution of (2) in Ω . This contradicts that v is a singular supersolution at x_0 . So the minimizers of $(v - u_\theta)$ are in $\partial\Omega \cup \Gamma_v$. The assertion is obtained by letting θ go to 1. \square

In the sequel, we assume that there exists a neighborhood A of $\partial\Omega$ and $\lambda > 0$ such that:

$$|H(x, p) - H(x, q)| \leq \lambda |p - q| \quad \forall x \in A, \quad \forall p, q \in \mathbb{R}^N. \quad (26)$$

In other words, we impose that H is Lipschitz continuous in p (with a Lipschitz constant which does not depend on $x \in A$) on a neighbourhood of $\partial\Omega$. Note that the SFS Hamiltonians H_{pers}^* and H_{orth}^* verify the hypothesis (26) (see [40]).

Using the maximum principle, we deduce the following strong uniqueness result:

Theorem 3 (Strong uniqueness of the SDVS with $\varphi = +\infty$ on $\partial\Omega$)

Let $u, v : \Omega \rightarrow \mathbb{R}$ be respectively an u.s.c. subsolution of (2)-(7), and a l.s.c. singular supersolution of (2)-(7), with φ verifying $\forall x \in \partial\Omega$, $\varphi(x) = +\infty$. If H verifies (26) then

$$\forall x \in \Omega, \quad u(x) \leq v(x). \quad (27)$$

PROOF. We consider $M = \max_{\overline{\Omega}} (u(x) - v(x))$. We argue by contradiction and assume that $M > 0$. By the maximum principle (Theorem 2), we have:

$$M = \max_{x \in \overline{\Omega}} (u(x) - v(x)) = \max_{x \in \partial\Omega \cup \Gamma_v} (u(x) - v(x)).$$

Let $x \in \Gamma_v$ and $y \in B_S(x)$ be such that $v(x) \geq \varphi(y) + \psi(x) - \psi(y)$. By (18) and because $\Gamma_v \subset \mathcal{S}$

$$v(x) \geq \varphi(y) + \psi(x) - \psi(y) \geq u(y) + \psi(x) - \psi(y) \geq u(x).$$

So, $\forall x \in \Gamma_v$, $u(x) - v(x) \leq 0$ and therefore

$$M = \max_{x \in \overline{\Omega}} (u(x) - v(x)) = \max_{x \in \partial\Omega} (u(x) - v(x)).$$

In other words, M is reached at a point $x_0 \in \partial\Omega$. Henceforth, we can work on a neighborhood A of the boundary $\partial\Omega$ where hypothesis (26) holds. By (5) we can assume that $A \cap \mathcal{S} = \emptyset$. So in this neighborhood A , the notion of singular viscosity solution coincides with the classical notion of discontinuous viscosity solutions. Therefore, we can obtain a contradiction exactly as in the proof of Theorem 4.6 of [3] (let us recall that we have assumed that H is coercive in p uniformly with respect to x). \square

More generally, we have the theorem:

Theorem 4 (Strong uniqueness of the SDVS) *Let $u, v : \Omega \rightarrow \mathbb{R}$ be respectively an u.s.c. subsolution of (2)-(7), and a l.s.c. singular supersolution of (2)-(7). Then*

$$\forall x \in \Omega, \quad u(x) \leq v(x).$$

PROOF. The statement can be proved combining the proofs of the previous theorem and of Theorem 4.5 (and of its Corollary 4.1) of Barles' book [3]. \square

Let us note that clearly the strong uniqueness involves the uniqueness on Ω of the singular viscosity solution of (2)-(7): i.e, if u_1 and u_2 are two singular viscosity solutions of (2)-(7), then $\forall x \in \Omega, u_1(x) = u_2(x)$. Moreover, it proves that this solution is continuous on Ω ($u = u^* = u_*$), therefore it is Lipschitz continuous on Ω (because subsolutions are Lipschitz continuous).

4.4 Stability of the singular solution

In this section, we show that the notion of SDVS enjoys some significative stability properties. This stability has important and appreciable consequences for the Shape from Shading problem.

4.4.1 A general stability result

We consider for $n \in \mathbb{N}$ the equations:

$$H_n(x, \nabla u) = 0, \quad \forall x \in \Omega \tag{28}$$

with continuous, convex and coercive Hamiltonians H_n satisfying (3)-(4).

We set for any $x \in \overline{\Omega}$:

$$\mathcal{Z}_n(x) = \{p \in \mathbb{R}^N \mid H_n(x, p) \leq 0\}$$

$$\mathcal{S}_n(x) = \{x \in \overline{\Omega} \mid H_n(x, \nabla \psi(x)) = 0\}.$$

We require the following conditions:

$$\text{there exists } M > 0 \text{ such that } \mathcal{Z}_n(x) \subset B(0, M) \text{ for any } x \in \overline{\Omega}, n \in \mathbb{N} \tag{29}$$

$$\theta_n \mathcal{Z}(x) + (1 - \theta_n) \nabla \psi(x) \subset \mathcal{Z}_n(x) \quad \text{for any } x \in \overline{\Omega}, n \in \mathbb{N} \tag{30}$$

$$H(x, p) \leq \liminf_{n \rightarrow +\infty} H_n(x, p) \quad \text{for any } (x, p) \in \overline{\Omega} \times B(0, M) \tag{31}$$

where θ_n is a sequence converging to 1.

REMARKS 8.

R8.1 - Assumption (29) implies that the SDVSs u_n of (28)-(7) verify $\|\nabla u_n\|_\infty \leq M$, for any n . So the functions u_n are uniformly Lipschitz continuous and also uniformly bounded on $\overline{\Omega}$.

R8.2 - By (9) and Remark 3, (30) involves

$$\mathcal{S}_n \subset \mathcal{S}$$

and

$$\theta_n S(x, y) \leq S_n(x, y), \quad \forall x, y \in \overline{\Omega},$$

where S_n is the distance defined as in (13) with $r_n(x) = \sup\{r > 0 \mid B(\nabla \psi(x), r) \subset \mathcal{Z}_n(x)\}$ in place of $r(\cdot)$. In particular, the topology τ_n is stronger than the topology τ .

We have the following stability result:

Theorem 5 (stability) *Let $u_n : \overline{\Omega} \rightarrow \mathbb{R}$ be a sequence of SDVS of (28)-(7) (with \mathcal{S}_n in place of \mathcal{S}) on $\overline{\Omega}$. Assume that (29)-(31) are satisfied. If u is the SDVS of (2)-(7), then*

$$u(x) = \lim_{n \rightarrow \infty} u_n(x)$$

uniformly in $\overline{\Omega}$.

PROOF. By (29) the sequence u_n is uniformly bounded and uniformly Lipschitz continuous in $\overline{\Omega}$. Hence, all the subsequences of $(u_n)_{n \in \mathbb{N}}$ converging toward $\limsup^* u_n$ and $\liminf_* u_n$ converge uniformly and $\limsup^* u_n$ and $\liminf_* u_n$ are bounded and Lipschitz continuous on $\overline{\Omega}$. By (31) it follows that $\limsup^* u_n$ is a viscosity subsolution of (2)-(7) (see for example [1], [2]).

If $\liminf_* u_n$ is a singular supersolution of (2)-(7), then by Theorem 4, we get

$$\limsup^* u_n \leq \liminf_* u_n.$$

Since the reverse inequality is true by definition we get that $\limsup^* u_n = \liminf_* u_n$ and therefore the sequence u_n converges uniformly toward the SDVS of (2)-(7). So, to conclude, it is sufficient to prove that all the limits u of subsequences of u_n uniformly convergent are singular supersolutions of (2)-(7):

1. Let $x_0 \in \mathcal{S}$ be such that $u(x_0) < \varphi(y) + \psi(x_0) - \psi(y)$ for any $y \in B_S(x_0)$, otherwise the conclusion is obvious. Note that, by continuity of u, φ and ψ , this inequality holds on a neighborhood of $B_S(x_0)$.

- By (30), we have

$$\rho_n(x, p) \leq \theta_n \rho(x, p) \tag{32}$$

for any $n \in \mathbb{N}$, $x \in \Omega$ and $p \in \mathbb{R}^N$.

- Assume for purpose of contradiction that there is a strict S -subtangent ϕ to u at x_0 which is also a strict viscosity subsolution of (2) in a neighborhood A of $B_S(x_0)$, i.e.

$$(u - \phi)(y) > (u - \phi)(x_0), \text{ for any } y \in A \setminus B_S(x_0),$$

$$\rho(y, \nabla \phi(y)) \leq \eta \tag{33}$$

in A in the viscosity sense, for some $\eta \in]0, 1[$.

- A standard argument in viscosity solution theory gives the existence of a sequence x_n of minimizer of $u_n - \phi$ verifying $S(x_0, x_n) \rightarrow 0$ (see [3], Lemma 4.2). By the uniform convergence of $(u_n)_{n \in \mathbb{N}}$, we have that $u_n(x_n) < \varphi(y) + \psi(x_n) - \psi(y)$ for any $y \in B_{S_n}(x_n) \subset B_S(x_n) \subset A$ for n sufficiently large. Hence, even if $x_n \in \mathcal{S}_n$, for n sufficiently large, u_n verifies at x_n the singular supersolution property. Since A is a neighborhood of $B_{S_n}(x_n)$, ϕ is S_n -subtangent to u_n at x_n .
- (32) and (33) involve:

$$\rho_n(y, \nabla \phi(y)) \leq \theta_n \eta, \quad \forall y \in A,$$

in viscosity sense. Hence ϕ is a strict subsolution of (28) for n large enough. This contradicts u_n being a singular supersolution of (28) at x_n .

2. If $x_0 \in \overline{\Omega} \setminus \mathcal{S}$ then $\rho(x, p) \geq 1$ if and only if $H(x, p) \geq 0$ and singular and discontinuous viscosity supersolution coincide. Hence the previous argument can be adapted to show that u is a viscosity supersolution also in this case.

□

4.4.2 Applications of the stability to the Shape from Shading

In computer vision, the images are always corrupted by noise. It is therefore very important to design schemes and algorithms *robust* to noise. That is to say we would like that the result obtained by the algorithm from a noisy image to be close to the ideal result obtained from the perfect image. Moreover, the computer vision algorithms use frequently various parameters. In this work, we assume that the camera is calibrated and that the position of the light source is known. So, for applying our algorithms, the user must input (as parameters) the focal length, the size of the pixels (width, height) and a vector representing the light source direction (following the chosen modeling). In practice, these additional data can be not known precisely and the inputs provided by the user can contain important errors. Consequently, to be applicable, the algorithms must be robust to these unavoidable errors on parameters. In other words, the returned results by the algorithms with corrupted parameters must be close to the results returned with the perfect theoretical parameters.

Mathematically, the robustness is expressed by the continuity of the application which from an image I (a focal length f or a light source direction \mathbf{L}, \dots , respectively), returns the solution u of the associated PDE. In other words, we would like that, for all sequences of noisy images I_n (of focal lengths f_n or of light source directions \mathbf{L}_n, \dots , respectively) converging toward an image I (f or \mathbf{L}, \dots , respectively), the sequence of recovered solutions u_n converges toward the solution u associated to I (f or \mathbf{L} , respectively). If we denote H_n the Hamiltonian obtained by replacing the parameters \mathbf{L} , f and I by \mathbf{L}_n , f_n and I_n in H , then the desired stability property corresponds with the convergence of the SDVSs of (28)-(7) towards the SDVS of (2)-(7) when $n \rightarrow +\infty$. In lots of cases, Theorem 5 allows to demonstrate that this property is satisfied.

In the sequel, we propose a way allowing to use Theorem 5 and to prove that such results hold for the Shape from Shading problem.

1. Approximation of the degenerated equations by non-degenerated equations:

The lack of uniqueness of the solution to (2) is a noteworthy problem for numerical computations of a solution to the Shape from Shading problem, since it causes numerical instability and sometimes fail of convergence of standard approximation schemes. It is therefore usual to regularize (2) by cutting the image intensity at a certain level strictly less than 1 before applying the approximation procedure. As a first application of Theorem 5, we show that the notion of SDVS is stable respect to this type of regularization. Given a continuous image I and $\varepsilon > 0$, we set⁴

$$I_\varepsilon(x) = \min(I(x), 1 - \varepsilon), \quad \forall x \in \overline{\Omega}.$$

For a SFS Hamiltonian H , we denote by H_ε the new Hamiltonian obtained replacing $I(x)$ by $I_\varepsilon(x)$ in H . Since $I_\varepsilon \leq I$, the reader will verify easily that for all the SFS Hamiltonians,

$$\forall x \in \overline{\Omega}, \quad \forall p \in \mathbb{R}^N, \quad H_\varepsilon(x, p) \leq H(x, p).$$

Therefore,

$$\forall x \in \overline{\Omega}, \quad \mathcal{Z}(x) \subset \mathcal{Z}_\varepsilon(x).$$

So the condition (30) holds for $\theta_\varepsilon = 1$. Moreover, it is easy to prove that H_ε converge toward H (when $\varepsilon \rightarrow 0$) uniformly with respect to $(x, p) \in \overline{\Omega} \times K$ for all compact set $K \subset \mathbb{R}^N$. Therefore, the singular viscosity solutions of (28)-(7) converge toward the unique singular viscosity solution of (2)-(7).

Now, let us remark that, $\forall \varepsilon > 0$, the SFS Hamiltonian H_ε (associated with I_ε) is not degenerate anymore (i.e $S = \emptyset$). So, its (unique) singular viscosity solution is the (unique) classical discontinuous viscosity solution. Thus, for approximating its solution, we can use the classical tools we have developed in [40].

2. Robustness of the Shape from Shading solutions to the image regularization:

In computer vision or more generally in image processing, the images are always corrupted by noise. To remove this noise, the images are often regularized [51]. In other respects, most of CCD sensors slightly smooth the images and defocus effects can strongly diffuse the brightness information [24]. Since, we do not have taken into account these regularization effects in the modeling, it seems important to guarantee the robustness of our SFS methods to them.

We consider a sequence of noisy (or denoised) images I_n converging uniformly to I and we set $\omega_n = \|I - I_n\|_{L^\infty(\Omega)}$.

Unfortunately, in this general situation, stability does not hold. It is possible to design counter examples for which I_n converges uniformly toward I but the corresponding SDVSs do not converge uniformly (see

⁴ Let us remind the reader that we assume that the intensity is between 0 and 1.

for example [6]). Here we show that if the images I_n are appropriately regularized, we recover again the stability of SDVSs.

Let ε_n be a sequence such that $\omega_n/\varepsilon_n \rightarrow 0$ for $n \rightarrow +\infty$. Set

$$I_{n\varepsilon_n} = \min(I_n(x), 1 - \varepsilon_n), \quad \forall x \in \overline{\Omega},$$

let $H_n(x, p)$ be the SFS Hamiltonians corresponding to the intensity $I_{n\varepsilon_n}$ and $Z_n = \{p \in \mathbb{R}^N : H_n(x, p) \leq 0\}$. For simplicity we assume that both the limit equation (2) and the regularized equations corresponding to the Hamiltonians H_n admit $\psi \equiv 0$ as a subsolution⁵. We want to show that assumption (30), with $\psi \equiv 0$, holds (the other assumptions of the stability theorem being obvious).

Set $\mathcal{S}^n = \{x \in \Omega : I(x) \geq 1 - \varepsilon_n\}$. We distinguish two cases

- (a) If $x \in \mathcal{S}^n$, then $I_{n\varepsilon_n}(x) \leq 1 - \varepsilon_n \leq I(x)$, hence, recalling that the SFS Hamiltonians are increasing in I , we get $Z(x) \subset Z_n(x)$.
- (b) If $x \notin \mathcal{S}^n$, then

$$\begin{aligned} I(x) &\geq I_n(x) - \omega_n \geq I_{n\varepsilon_n}(x) - \omega_n = I_{n\varepsilon_n}(x) - \frac{\omega_n}{\varepsilon_n} \varepsilon_n \geq \\ &I_{n\varepsilon_n}(x) - \frac{\omega_n}{\varepsilon_n} (I_{n\varepsilon_n}(x) - 1) \geq (1 - \frac{\omega_n}{\varepsilon_n}) I_{n\varepsilon_n}(x). \end{aligned}$$

Therefore, recalling that $\omega_n/\varepsilon_n \rightarrow 0$, we find that hypothesis (30) is satisfied with $\theta_n = (1 - \frac{\omega_n}{\varepsilon_n})^{-1}$.

EXAMPLE : A typical example of a denoised sequence of images is given by $I_n(x) = (I * \eta_n)(x)$, where η_n is a standard mollifier, i.e. $\eta_n(x) = n^N \eta(nx)$ with $\eta : \mathbb{R}^N \rightarrow \mathbb{R}$ a smooth, nonnegative function such that the support of η is contained in the unit ball and $\int_{\mathbb{R}^N} \eta(z) dz = 1$ (we assume for simplicity that I is defined in a neighborhood of $\overline{\Omega}$, so I_n can be defined in $\overline{\Omega}$ for n sufficiently large). I_n is a smooth function and $0 \leq I_n(x) \leq 1$. Moreover $I_n(x) = 1$ if and only if $I(y) = 1$ for any $y \in B(x, 1/n)$. Hence $\mathcal{S}_n = \{x \in \Omega : I_n = 1\}$ is a proper subset of \mathcal{S} . If \mathcal{S} reduces for example to a finite number of points, the regularized problem is not singular. Note that H_n satisfies the same hypothesis of H , i.e. it is continuous, convex and, since $I \geq m > 0$ implies $I_n \geq m > 0$, also coercive in p .

3. Robustness of the Shape from Shading solutions to pixel noise and errors on parameters:

Now we consider the case, where \mathbf{L}_n and f_n converge toward \mathbf{L} and f (here, we fix $I_n = I$). Up to a change of variables, we assume that $\psi = 0$. For a maximum of generality, we deal with the generic SFS Hamiltonian.

- (a) Let us recall that the classical SFS Hamiltonians are special cases of the generic SFS Hamiltonian

$$H_g(x, p) = \kappa_x \sqrt{|A_x p + \mathbf{v}_x|^2 + K_x^2} + \mathbf{w}_x \cdot p + c_x$$

where $\kappa_x, A_x, \mathbf{v}_x, K_x, \mathbf{w}_x$ and c_x are completely described in section 3.3.2 of [40]. For all SFS Hamiltonians, the functions $\kappa_x, A_x, \mathbf{v}_x, K_x, \mathbf{w}_x$ and c_x depend continuously on x, \mathbf{L} and f (see appendix B of [40] for details). Let us denote \mathbf{L}_n and f_n the approximations of \mathbf{L} and f . $\kappa_x^n, A_x^n, \mathbf{v}_x^n, K_x^n, \mathbf{w}_x^n, c_x^n$ the approximations of $\kappa_x, A_x, \mathbf{v}_x, K_x, \mathbf{w}_x, c_x$ obtained by replacing \mathbf{L} and f by \mathbf{L}_n, f_n . H_n is the approximation of H_g .

- (b) Let us remind that the notion of SDVS requires the coercivity of the Hamiltonians. So we assume that there exists $\delta > 0$ such that

$$\forall x \in \overline{\Omega}, \quad \kappa_x - |{}^t A_x^{-1} \mathbf{w}_x| > \delta$$

(see proposition 2 of [40]). If we assume that $\mathbf{L}_n \rightarrow \mathbf{L}$ and $f_n \rightarrow f$ then for all SFS Hamiltonians, we have by continuity: for all n large enough,

$$\forall x \in \overline{\Omega}, \quad \kappa_x^n - |({}^t A_x^n)^{-1} \mathbf{w}_x^n| > \frac{\delta}{2}$$

⁵ Let us recall that by an appropriate change of variables, the SFS Hamiltonians $H_{P/F}^{pers}$ and $H_{R/T}^{orth}$ can be reduced to this case.

so, the functions H_n are coercive in p uniformly with respect to $x \in \overline{\Omega}$ and $n \in \mathbb{N}$. In particular, the hypothesis (29) holds.

- (c) For all $x \in \overline{\Omega}$ and $p \in S^2$ (the unit sphere in \mathbb{R}^2), let us consider $g : \Omega \times \mathbb{R}^+ \rightarrow \mathbb{R}$ defined by

$$g(x, r) = H(x, \nabla\psi + rp)$$

and g_n the approximation of g designed from H_n (instead of H). Clearly, there exist $a(x, p)$, $b(x, p)$, $c(x, p)$, $\mu(x, p)$ and $\nu(x, p)$ in \mathbb{R} such that

$$g(x, r) = \kappa_x \sqrt{a(x, p)r^2 + b(x, p)r + c(x, p)} + \mu(x, p)r + \nu(x, p).$$

Obviously, we have the same rewriting of g_n with a_n , b_n , c_n , μ_n and ν_n which are the appropriate approximations. The uniform coercivity of the functions H_n and function H involves that there exists $\delta > 0$ such that $\forall x \in \overline{\Omega}$, $p \in S^N$, $n \in \mathbb{N}$,

$$(\kappa_x^n)^2 a_n(x, p) - \mu_n(x, p)^2 > \delta \quad \text{and} \quad \kappa_x^2 a(x, p) - \mu(x, p)^2 > \delta.$$

Since $\psi = 0$ is a subsolution, we have

$$(\kappa_x^n)^2 c_n(x, p) - \nu_n(x, p)^2 \leq 0 \quad \text{and} \quad \kappa_x^2 c(x, p) - \nu(x, p)^2 \leq 0$$

with a strict inequality outside of \mathcal{S} (note that since $I_n = I$ then $\mathcal{S}_n = \mathcal{S}$).

Note that ν and ν_n are non positive.

So, by using the appendix C.4 of [40], we can claim that for $x \notin \mathcal{S}$, the equation $g(x, r) = 0$ has a unique solution in \mathbb{R}^+ ⁶. It is given by:

$$r(x, p) = \frac{-(\kappa_x^2 b(x, p) - 2\mu(x, p)\nu(x, p)) + \sqrt{\Delta(x, p)}}{2(\kappa_x^2 a(x, p) - \mu(x, p)^2)}$$

where

$$\Delta(x, p) = (\kappa_x^2 b(x, p) - 2\mu(x, p)\nu(x, p))^2 - 4(\kappa_x^2 c(x, p) - \nu(x, p)^2)(\kappa_x^2 a(x, p) - \mu(x, p)^2).$$

Of course, the same result holds for the equation $g_n(x, r) = 0$. We denote $r_n(x, p)$ its solution. By using the adequate approximations, we obtain the same expression as $r(x, p)$.

- (d) For all $x \in \overline{\Omega} \setminus \mathcal{S}$ and $p \in S^2$, let us denote

$$\theta_n(x, p) = \frac{r_n(x, p)}{r(x, p)}.$$

If (x, p) is fixed in $\overline{\Omega} \setminus \mathcal{S} \times S^2$, then we have $\theta_n(x, p) \rightarrow 1$, when $n \rightarrow +\infty$. As we explain in the sequel, the conclusion follows as soon as we have proved that this convergence is uniform. In the following example, we show that, with a few additional regularity hypotheses (for example, $I \in C^1(\overline{\Omega})$), this step can be done by considering some precise SFS Hamiltonians. But this step is not obvious because $r(x, p)$ and $r_n(x, p)$ vanishes on \mathcal{S} . Also, we do not have find a generic proof.

- (e) Now let us prove that the conclusion follows as soon as $\theta_n(x, p) \rightarrow 1$ uniformly when $n \rightarrow +\infty$.

Let us denote

$$\underline{\theta}_n = \min_{(x, p) \in \overline{\Omega} \setminus \mathcal{S} \times S^N} \theta_n(x, p),$$

we have $\underline{\theta}_n \rightarrow 1$ when $n \rightarrow +\infty$. In other respects, by hypothesis (4), we have:

$$\forall x \in \overline{\Omega}, \forall q \in \tilde{\mathcal{Z}}(x) = \mathcal{Z}(x) - \nabla\psi(x), \quad \exists \mu \geq 1 \text{ such that } \mu q \in \partial \tilde{\mathcal{Z}}(x).$$

By definition of $\theta_n(x, p)$, we have

$$\theta_n \left(x, \frac{q}{|q|} \right) (\mu q) \in \partial \tilde{\mathcal{Z}}_n(x).$$

⁶Let us fix x in $\overline{\Omega} \setminus \mathcal{S}$. For all our SFS Hamiltonians we have $\psi(x) = \argmin_p H(x, p)$ and $H(x, \nabla\psi(x)) < 0$. So, by continuity, coercivity and convexity of H , for all $p \neq 0$, the equation (in $r \in \mathbb{R}$) $H(x, \nabla\psi + rp) = 0$ has two solutions: a positive one and a negative one. The positive solution is the largest...

Since $0 \leq \underline{\theta}_n \leq \mu \theta_n \left(x, \frac{q}{|q|}\right)$, the hypothesis (4) involves

$$\underline{\theta}_n q \in \tilde{\mathcal{Z}}_n(x) = \mathcal{Z}_n(x) - \nabla \psi(x).$$

Thus, we have proved $\forall x \in \overline{\Omega}$,

$$\underline{\theta}_n \tilde{\mathcal{Z}}(x) \subset \tilde{\mathcal{Z}}_n(x).$$

So,

$$\underline{\theta}_n \mathcal{Z}(x) + (1 - \underline{\theta}_n) \nabla \psi \subset \mathcal{Z}_n(x).$$

So the hypothesis (30) holds.

Let us remind that above, we have shown that in general the hypotheses (29) also holds with the SFS equations (when the focal length, the light source direction (...) are corrupted and when errors vanish). (31) clearly holds. Therefore, theorem 5 applies. The stability is then proved.

EXAMPLE : Let us consider the example of the Hamiltonian $H_{D/O}^{orth}$ with $\mathbf{L}_n \rightarrow \mathbf{L}$. So

$$H(x, p) = I(x) \sqrt{1 + |p|^2 - 2p \cdot \mathbf{l}} + p \cdot \mathbf{l} - 1$$

and

$$H_n(x, p) = I(x) \sqrt{1 + |p|^2 - 2p \cdot \mathbf{l}_n} + p \cdot \mathbf{l}_n - 1.$$

Easily, one can verify that

$$r(x, p) = \sqrt{1 - I(x)^2} \frac{I(x) \sqrt{1 - (p \cdot \mathbf{l})^2} - (p \cdot \mathbf{l}) \sqrt{1 - I(x)^2}}{I(x)^2 - (p \cdot \mathbf{l})^2},$$

and that $\forall x \in \overline{\Omega}$, $\forall p \in S^N$,

$$\theta_n(x, p) = \frac{I(x) \sqrt{1 - (p \cdot \mathbf{l}_n)^2} - (p \cdot \mathbf{l}_n) \sqrt{1 - I(x)^2}}{I(x) \sqrt{1 - (p \cdot \mathbf{l})^2} - (p \cdot \mathbf{l}) \sqrt{1 - I(x)^2}} \cdot \frac{I(x)^2 - (p \cdot \mathbf{l})^2}{I(x)^2 - (p \cdot \mathbf{l}_n)^2}.$$

If the brightness image I is differentiable and if ∇I is bounded on $\overline{\Omega}^7$ then, $\partial_x \theta_n(x, p)$ is bounded independently of $x \in \overline{\Omega}$, $n \in \mathbb{N}$ and p on a neighborhood of S^N .

PROOF. Let us denote $s_n = p \cdot \mathbf{l}_n$ and $s = p \cdot \mathbf{l}$.

Note that $s_n \rightarrow s$ uniformly with respect to p in a neighborhood of S^N .

Let us consider the function

$$\begin{aligned} T : \mathbb{R} &\rightarrow \mathbb{R} \\ X &\mapsto \frac{\sqrt{1 - s_n} X - s_n \sqrt{1 - X^2}}{\sqrt{1 - s} X - s \sqrt{1 - X^2}}. \end{aligned} \quad (34)$$

$\forall \delta > 0$ (and small enough), we have for all n large enough, $|s_n| < |s| + \delta \leq 1$, T is continuously derivable on $[s + \delta, 1]$ and T' is bounded independently of s_n ⁸.

By the uniform coercivity assumption, there exists $\delta > 0$ such that for all p in a neighborhood of S^N and for all n large enough,

$$|s_n| < |s| + \delta < \min_{x \in \overline{\Omega}} I(x) \leq 1.$$

Since,

$$\nabla_x (T \circ I)(x) = T'(I(x)) \nabla_x I(x),$$

therefore $\nabla_x (T \circ I)$ is bounded independently of x, p and n . We can conclude by using the fact that the function

$$x \mapsto \frac{I(x)^2 - (p \cdot \mathbf{l})^2}{I(x)^2 - (p \cdot \mathbf{l}_n)^2}$$

⁷ for example, since Ω is bounded, ∇I is bounded as soon as $I \in C^1(\overline{\Omega})$.

⁸ so independently of n and p in a neighborhood of S^N .

and its gradient are bounded independently of x in $\overline{\Omega}$, n in \mathbb{N} and p in a neighborhood of S^N . \square

In a same way, we prove that $\partial_p \theta_n(x, p)$ is uniformly bounded. Let us denote $X = (x, p)$. So we have $\nabla_X \theta_n(X)$ uniformly bounded. Moreover,

$$\forall X, Y \in \overline{\Omega} \times S^N, \quad |\theta_n(X) - \theta_n(Y)| \leq |\nabla_X \theta_n|_\infty L(X, Y),$$

where $L(X, Y)$ is the Euclidean geodesic distance in $\Omega \times S^N$. Also, it is well known [31] that for any fixed $X \in \overline{\Omega}$, $Y \mapsto L(X, Y)$ is *Lipschitz continuous* in $\overline{\Omega} \times S^N$ and that the Lipschitz constant does not depend with respect to X . Thus the functions θ_n are uniformly Lipschitz continuous. Therefore the convergence of the sequence θ_n is uniform.

REMARK 9. In a general way, the above development is not systematically applicable when the images are noised and the corrupted images I_n converge toward I . For example, let us consider the Hamiltonian $H_{D/O}^{orth}$ with $I_n \rightarrow I$ and $\mathbf{L} = (0, 0, 1)$. So

$$H(x, p) = I(x) \sqrt{1 + |p|^2} - 1$$

and

$$H_n(x, p) = I_n(x) \sqrt{1 + |p|^2} - 1.$$

$\forall x \in \overline{\Omega} \setminus \mathcal{S}$, $\forall p \in S^N$, we have

$$\theta_n(x, p) = \frac{I(x)}{I_n(x)} \frac{\sqrt{1 - I_n(x)^2}}{\sqrt{1 - I(x)^2}}.$$

5 A general framework for SFS

In this section, we explain *why the notion of state constraints is relevant* when we do not know the values of the solution and we describe this boundary condition in a more intuitive way. Moreover, we show that *the notion of SDVS provides a general mathematical framework unifying the previous mathematical frameworks* based on viscosity solution theory proposed in the SFS literature.

The main contribution of the notion of SDVS lies in the possibility to impose the heights of the solution at the singular points when we know them⁹ and on the possibility to “send to infinity” the boundary conditions when we do not know them. This possibility also holds for all the points located on the boundary of the image $\partial\Omega$. Let us recall that in the previous work [45, 43, 41, 40, 10, 22, 23], the various notions of viscosity solutions [continuous, discontinuous or singular] are used with (finite) Dirichlet conditions on the boundary of the images. Note that, in [32], Lions et al. have already used the notion of states constraints, but they used it only to deal with apparent contours and in the eikonal setup. More precisely, they use it only at the points $x \in \partial\Omega$ such that $I(x) = 0$ and “ $\frac{\partial u}{\partial n} = -\infty$ ”. Here, we use the state constraints at each point of $\partial\Omega \cup \mathcal{S}$, where we do not know the value of the solution.

Let us focus on the points on the boundary $\partial\Omega$ of the image. For simplicity, let us assume that we know the values of the solution at all the singular points. First, in contrast with the Dirichlet and Neumann boundary conditions, the state constraints are interesting because they do not require any data. Let us recall that the Dirichlet (respectively, Neumann) boundary conditions require the knowledge of the values of the solution (respectively, the values of $\nabla u(x) \cdot n(x)$, where $n(x)$ is the unit inward normal vector to $\partial\Omega$ at the point x) on the boundary of the domain. But, in general, we rarely have such data at our disposal. Second, the notion of state constraints is also interesting because it provides a relevant solution as soon as the image is yielded by a “surface” u which verifies the supersolution constraint on $\partial\Omega$. Also, as we explain below, this constraint is

⁹ This is impossible with discontinuous viscosity solutions; see the second part of section 3.5.3 of [40]. It is possible with continuous viscosity solutions but compatibility conditions are required. In [10, 22, 23], Falcone et al. “send” systematically the singular points “at the infinity”.

very weak and it is commonly verified with real observable surface. Recall that an equivalent way to define the viscosity supersolution constraint at a point $x \in \partial\Omega$ is to require that

$$H(x, \xi) \geq 0, \quad \forall \xi \in D^-u(x) \quad (35)$$

where

$$D^-u(x) = \left\{ \xi \in \mathbb{R}^N \mid \liminf_{y \rightarrow x, y \in \bar{\Omega}} \frac{u(y) - u(x) - \xi(y - x)}{|y - x|} \geq 0 \right\}$$

(see for example [3, 1, 14]). This constraint can be roughly interpreted as following: *For all plan P sub tangent to u at x , the gradient ∇P verifies $H(x, \nabla P) \geq 0$.* To better understand the constraint (35) for x in $\partial\Omega$, let us consider the particular case of a differentiable solution.

Proposition 6 *Let u be a solution differentiable on $\bar{\Omega}$ of the HJB equation associated with the Hamiltonian*

$$H(x, p) = \sup_{a \in A} \{-f(x, a) \cdot p - l(x, a)\}. \quad (36)$$

and denote by $a_0(u, x)$ the optimal control of (36) associated to u at the point x (i.e. $a_0(u, x)$ is the control $a \in A$ maximizing $-f(x, a) \cdot \nabla u(x) - l(x, a)$). If for $x \in \partial\Omega$,

$$f(x, a_0(u, x)) \cdot n(x) > 0, \quad (37)$$

where $n(x)$ is the unit inward normal vector to $\partial\Omega$ at the point x , then (35) is satisfied.

In other words, the surface u is a supersolution on $\partial\Omega$ (i.e. u verifies the state constraints on $\partial\Omega$) as soon as the *dynamic of the optimal control* (associated with u) *points inward* of Ω at all points x on the boundary $\partial\Omega$. In the classical example of the *Eikonal equation*, the optimal control associated to a differentiable function u is

$$f(x, a_0(u, x)) = -a_0(u, x) = -\frac{\nabla u(x)}{|\nabla u(x)|}.$$

So in this example, u is a supersolution on $\partial\Omega$ as soon as for all x on $\partial\Omega$, the gradient $\nabla u(x)$ points outward of Ω , i.e. roughly speaking, when $u(x)$ “increases” when x come up to $\partial\Omega$. More generally, (37) can be globally interpreted as “ $u(x) - \psi(x)$ increases when x come up to $\partial\Omega$ ”.

In other respects, let us note that proposition 6 shows that the notion of state constraints coincides with the constraint formulated by Dupuis and Oliensis in assumption 2.1 of [20] and introduced in the case of solutions C^1 .

PROOF OF PROPOSITION 6. Let $x \in \partial\Omega$ be such that (37) is satisfied. We have for $c \leq 0$

$$\begin{aligned} H(x, \nabla u(x) + cn(x)) &= H(x, \nabla u(x) + cn(x)) - H(x, \nabla u(x)) \geq \\ &= -f(x, a_0(x, u)) \cdot (\nabla u(x) + cn(x)) - l(x, a_0(x, u)) - (-f(x, a_0(x, u)) \cdot \nabla u(x) - l(x, a_0(x, u))) \\ &= -f(x, a_0(x, u)) \cdot cn(x) \geq 0 \end{aligned}$$

Moreover, since u is differentiable on $\bar{\Omega}$, we have

$$D^-u(x) = \{\xi \mid \xi = \nabla u(x) + cn(x), \ c \leq 0\}.$$

Thus, for any $\xi \in D^-u(x)$,

$$H(x, \xi) \geq 0.$$

So the constraint (35) holds. \square

Now, *let us focus on the singular points.* We denote by Π_u the set of points in Ω such that a constant function cannot be S -subtangent to $u - \psi$ at x . If $x \notin \mathcal{S}$ or $B_S(x) = \{x\}$, this means that x cannot be a local minimum point for $u - \psi$. For this reason we call Π_u the set of minimum points of $u - \psi$. We also set

$$\Gamma_u = \{x \in \Omega \mid \exists y \in B_S(x) \text{ verifying } u(x) \geq \varphi(y) + \psi(x) - \psi(y)\}.$$

Theorem 6 *Let u be a (discontinuous) viscosity solution of (2)-(7) such that $u(x) \leq \varphi(x)$ for any $x \in \mathcal{S}$. If $\Pi_u \subset \Gamma_u$ then u is the SDVS of (2)-(7).*

In other words, the SDVS is the unique (discontinuous) viscosity solution u of (2)-(7) (verifying $\forall x \in \mathcal{S}, u(x) \leq \varphi(x)$) without local minima on $\Omega \setminus \Gamma_u$. Of course, the reciprocal statement of Theorem 6 holds. That is to say that the SDVS cannot have points of local minimum (in Ω) outside of Γ_u . In effect, by contradiction, if $u - \psi$ admits a constant function S -subtangent to $x_0 \notin \Gamma_u$, then the function ψ is a S -subtangent to u at x_0 . Since by the definition of \mathcal{S} , ψ is a strict subsolution of (2) it follows that u cannot be a (singular) supersolution at x_0 .

An important interpretation and consequence of Theorem 6 is the following:

The (discontinuous) viscosity solutions of (2)-(7) can be characterized only by their minima.

That is to say, if u is a (discontinuous) viscosity solutions of (2)-(7) then u is the (unique) SDVS of

$$\begin{cases} H(x, \nabla u) = 0, & \forall x \in \Omega, \\ u(x) = \hat{\varphi}(x), & \forall x \in \partial\Omega \cup \mathcal{S}, \end{cases}$$

where

$$\begin{aligned} \hat{\varphi}(x) &= \varphi(x), & \forall x \in \Pi_u \cup \partial\Omega, \\ \hat{\varphi}(x) &= +\infty, & \forall x \in \mathcal{S} \setminus \Pi_u. \end{aligned}$$

Thus this result extends consistently the work of Dupuis and Oliensis [20]. In [20], Dupuis and Oliensis characterize the C^1 solutions by their values at the local minimum points¹⁰. Here, we have extended this characterization to the (discontinuous) viscosity solutions.

PROOF OF THEOREM 6. We have just to prove that the solution u is a singular supersolution at all the singular points which are not in Γ_u . We assume for simplicity that $B_S(x_0) = \{x_0\}$ but it is straightforward to extend the argument to the general case.

We argue by contradiction assuming that there exists a function ϕ , a neighborhood $A \subset \Omega \setminus \Gamma_u$ of x_0 and $\theta \in]0, 1[$ such that ϕ is a S -subtangent to u at x_0 with

$$\begin{aligned} \phi(x_0) &= u(x_0), \\ \phi(x) &\leq u(x), & x \in A, \\ \phi(x) &\leq u(x) - \eta, & x \in \partial A \end{aligned}$$

for some $\eta > 0$ and

$$\rho(x, \nabla \phi) \leq \theta \quad x \in A$$

in the viscosity sense. Since u is a solution of (2) in A we have (see [31, 1])

$$u(x) = \psi(x) + \min\{u(y) - \psi(y) + L_A(x, y) : y \in \partial A\} \wedge \{u(x_0) - \psi(x_0) + L_A(x, x_0)\}. \quad (38)$$

Since x_0 is not a minimum point of $u - \psi$, we can find x_n such that $L(x_n, x_0) \rightarrow 0$ for $n \rightarrow \infty$ and $u(x_n) - \psi(x_n) \leq u(x_0) - \psi(x_0)$. It follows that $u(x_0) - \psi(x_0) + L_A(x_n, x_0) > u(x_n) - \psi(x_n)$ (since $L_A(x_n, x_0) > 0$). By (38), we can find $y_n \in \partial A$ such that $u(x_n) = \psi(x_n) + u(y_n) - \psi(y_n) + L_A(x_n, y_n)$. Hence

$$\begin{aligned} 0 &\geq u(y_n) - \psi(y_n) - u(x_0) + \psi(x_0) + L_A(x_n, y_n) - L_A(x_n, x_0) \geq \\ &\phi(y_n) + \eta - \psi(y_n) - \phi(x_0) + \psi(x_0) + L_A(x_n, y_n) - L_A(x_n, x_0). \end{aligned} \quad (39)$$

Passing to a subsequence we can assume that $y_n \rightarrow y_0$ with $y_0 \in \partial A$. Since $L_A(x_n, y_n)$ and $L_A(x_0, y_n)$ converge to $L_A(x_0, y_0)$ and $L_A(x_n, x_0)$ converges to 0, we can find n large such that

$$L_A(x_n, y_n) - L_A(x_n, x_0) + \eta > L_A(x_0, y_n).$$

Substituting the previous inequality in (39) we get

$$0 > \phi(y_n) - \psi(y_n) - \phi(x_0) + \psi(x_0) + L_A(x_0, y_n).$$

¹⁰ Let us recall that in [20], the functional cost l had to be positive. This is why Dupuis and Oliensis need to introduce the SFS Hamiltonian $H_{D/O}^{orth}$ (instead of dealing with $H_{R/T}^{orth}$). Here, we relax this constrained assumption.

Fixed such n , we can find $\xi \in W^{1,\infty}([0, 1], \overline{A})$ joining x_0 to y_n satisfying

$$\int_0^1 \left(\delta(\xi(t), -\dot{\xi}(t)) + \frac{d}{dt}(\phi(\xi(t)) - \psi(\xi(t))) \right) dt < 0.$$

From the previous inequality we get a contradiction to the definition of singular viscosity supersolution as in the proof of Theorem 1. \square

Finally, let us emphasize that the notion of SDVS allows to *unify* the various theories based on viscosity solutions used for solving the SFS problem. In effect,

- in the case where the Dirichlet Boundary Conditions (DBC) are finite on $\partial\Omega \cup \mathcal{S}$ and the compatibility condition (see [31]) holds, then the SDVS of (2)-(7) is the continuous viscosity solution used by [45, 32, 43, 41];
- in the case where the DBC are finite on $\partial\Omega$ and where there do not exist singular points, then the SDVS of (2)-(7) coincides with the discontinuous viscosity solution used by [41, 40, 42] (the compatibility conditions are no more required);
- when the DBC are finite on the boundary of the image and state constraints are imposed at the singular points, the SDVS of (2)-(7) corresponds to the Camilli and Siconolfi's singular viscosity solutions [11, 9, 12] used by Falcone et al. [10, 22, 23];
- as we have demonstrated above the SDVSs coincide with the C^1 solutions of (2) verifying the assumption 2.1 of Dupuis and Oliensis (when smooth solutions exist). Therefore, when there do not exist C^1 solutions¹¹, the notion of SDVS allows to extend consistently the work of Dupuis and Oliensis [20].

As a consequence, all the theoretical results of Falcone et al. [10, 22, 23]¹², Rouy et al. [45, 32]¹³, Prados et al. [43, 41]¹⁴ and Dupuis et al. [20]¹⁵ are *automatically extended to the “perspective SFS”* (use H_F^{pers} and $H_{P/F}^{pers}$).

Finally, one can conjecture that by using the work of [29, 38, 49, 13], the notion of SDVS can be extended to solve SFS problem with discontinuous images. This would be very difficult without the tool of viscosity solutions.

6 Minimal and global viscosity solutions

The SDVS allows to send the boundary conditions at $+\infty$; thereby obtaining the “maximal” solution. So for obtaining the “minimal” solution, it can seem natural to send them at $-\infty$. Nevertheless with such boundary conditions there do not exist solutions. In other respects, the viscosity solutions of the equation $H(x, \nabla u) = 0$ are different from the viscosity solutions of $-H(x, \nabla u) = 0$. For example, the opposite two equations on $]0, 1[$ associated with $H_1(x, p) = |p| - 1$ constrained by $u(0) = u(1) = 0$ have a unique viscosity solution given by figure 3. By schematizing, the solution of $H(x, \nabla u) = 0$ allows upward kinks whereas $-H(x, \nabla u) = 0$ allows downward kinks. Moreover, it is well known that:

$$[u \text{ solution of } -H(x, p)] \iff [-u \text{ solution of } H(x, -p)].$$

Thus it is natural to define the “minimal” solution of $H(x, p)$ by the opposite of the SDVS of $H(x, -p)$. Obviously, the Hamiltonians $H(x, -p)$ associated with all the SFS Hamiltonians are particular cases of the generic SFS Hamiltonian. Therefore all the previous theoretical and algorithmic results hold for the “minimal” SFS solutions. The interest of the notion of the “minimal” solution is twofolds: first it allows to recover surface which are “globally” concave (whereas SDVSs are “globally” convex). The second interest of these “minimal” solutions lies on a possible extension of the “global algorithm” of Oliensis [37, 20].

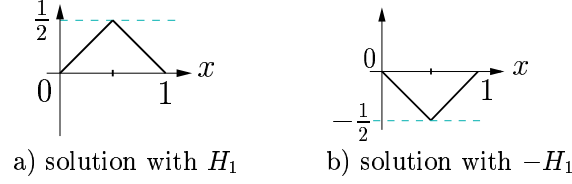
¹¹ Let us recall that, because of noise, of errors on parameters (focal length, light position, etc) and of incorrect modeling (interreflections, nonpunctual light source, nonlambertian reflectance...) there never exist such smooth solutions in practice.

¹² Who only deal with “orthographic Shape from Shading”.

¹³ Who only deal with “orthographic SFS” by using $H_{R/T}^{orth}$.

¹⁴ Who deal with $H_{R/T}^{orth}$ and $H_{P/F}^{pers}$.

¹⁵ Who only deal with “orthographic SFS” by using $H_{D/O}^{orth}$.

Figure 3: solutions of H versus $-H$; minimal solutions

7 Numerical approximation of the SDVS for generic SFS

This section explains how to compute a numerical approximation of the SDVS of the generic SFS equation. This requires three steps. First we “regularize” the equation. Second, we approximate the “regularized” SFS equation by approximation schemes. Finally, from the approximation schemes, we design numerical algorithms.

7.1 Management of the state constraints

In this section, we explain how to deal with the state constraints *in practice*. In particular, we show that, in the setup of this paper, the state constraints can always be rewritten by as Dirichlet boundary conditions. Let u be the SDVS of equation (2)-(7):

$$\begin{cases} H(x, \nabla u) = 0 & \forall x \in \Omega, \\ u(x) = \varphi(x) & \forall x \in \partial\Omega \cup \mathcal{S} \end{cases}$$

In section 4, we have seen that u is Lipschitz continuous and then bounded on Ω . Let $M \in \mathbb{R}$ an upper bound of u on Ω such that

$$\forall x \in \Omega, \quad u(x) < M - 1.$$

Now, let us consider $\tilde{\varphi}$ the real function defined on $\partial\Omega \cup \mathcal{S}$ by

$$\tilde{\varphi}(x) = \min(M, \varphi(x)),$$

and let \tilde{u} be the SDVS of equation

$$\begin{cases} H(x, \nabla u) = 0 & \forall x \in \Omega, \\ u(x) = \tilde{\varphi}(x) & \forall x \in \partial\Omega \cup \mathcal{S}. \end{cases}$$

Following these notations, we have

Proposition 7 \tilde{u} and u coincide on Ω , i.e.

$$\forall x \in \Omega, \quad \tilde{u}(x) = u(x).$$

PROOF. Thank to the strong uniqueness of the SDVS (theorem 3), it is sufficient to prove that \tilde{u} is an SDVS of (2)-(7). Let us recall that the uniqueness of the SDVS only holds on Ω but not on $\overline{\Omega}$. Also, \tilde{u} and u can take different values at some points of $\partial\Omega$.

First, since $\tilde{\varphi} \leq \varphi$, by the maximum principle (theorem 2) we have,

$$\forall x \in \Omega, \quad \tilde{u}(x) \leq u(x).$$

• \tilde{u}^* is a subsolution of (2)-(7):

- \tilde{u}^* is a subsolution of (2) on $\Omega \setminus \mathcal{S}$;
- for all x_0 in $\partial\Omega \cup \mathcal{S}$ such that $\tilde{u}^*(x_0) \leq \tilde{\varphi}(x_0)$ we have trivially $\tilde{u}^*(x_0) \leq \varphi(x_0)$.
- for all x_0 in $\partial\Omega$ such that $\tilde{u}^*(x_0) > \tilde{\varphi}(x_0)$, \tilde{u}^* verifies the subsolution property.

- \tilde{u}_* is a supersolution of (2)-(7):
 - \tilde{u}_* is a supersolution of (2) on $\Omega \setminus \mathcal{S}$;
 - Let $y \in \partial\Omega \cup \mathcal{S}$ be a point such that $\tilde{u}_*(y) \geq \tilde{\varphi}(y) = \min(\varphi(y), M)$. So $\tilde{u}_*(y) \geq M$ or $\tilde{u}_*(y) \geq \varphi(y)$. But $\tilde{u}_*(y) \geq M$ is impossible (because, for all $z \in \Omega$, $\tilde{u}(z) \leq u(z) < M - 1$, then for all $y \in \overline{\Omega}$ $\tilde{u}_*(y) \leq M - 1 < M$). Therefore $\tilde{u}_*(y) \geq \varphi(y)$.
 - Let $x_0 \in \partial\Omega \cup \mathcal{S}$. If there exist $y \in B_S(x_0)$ such that $\tilde{u}_*(y) \geq \tilde{\varphi}(y)$. then by the previous item, $\tilde{u}_*(y) \geq \varphi(y)$. Else, the singular viscosity property holds for \tilde{u}_* at x_0 . Therefore \tilde{u}_* is a supersolution of (2)-(7) for all points $x_0 \in \partial\Omega \cup \mathcal{S}$.

□

Therefore, equations (2)-(7) with some state constraints (i.e. such that for some $x \in \partial\Omega \cup \mathcal{S}$ $\varphi(x) = +\infty$) can be rewritten as equations without state constraints; i.e. with (finite) Dirichlet boundary conditions on the whole set $\partial\Omega \cup \mathcal{S}$. So in practice, we always consider (finite) Dirichlet boundary conditions: when we know the values of the solution on $\partial\Omega$ we can transfer these informations in φ ; when we do not have these data and we want to compute the solution of with state constraints, we impose φ to be a “great” *constant*. Let us emphasize that by modifying φ in such a way, we do not change the solution of (2)-(7) neither the approximation computed by our algorithm.

7.2 Regularization of the generic SFS equation

For an intensity image I and $\varepsilon > 0$, let us consider the truncated image I_ε defined by $I_\varepsilon(x) = \min(I(x), 1 - \varepsilon)$. By using the stability result of theorem (5), we have proved in section 4.4.2-1 that for all SFS Hamiltonians, the classical discontinuous viscosity solution¹⁶ associated with the image I_ε converges uniformly toward the singular viscosity solution associated with the image I , when $\varepsilon \rightarrow 0$. Thus for approximating this equation, we can use the classical tools developed by Barles and Souganidis [5].

7.3 Approximation schemes for the nondegenerate SFS equations

Let us consider the “regularized” generic SFS equation. In [40], we have designed SFS monotonous approximation schemes which are always stable (existence of a solution). Moreover, we also prove in [40] that (as soon as the intensity image is Lipschitz continuous and the Hamiltonian is coercive) the solutions of these schemes converge toward the unique (classical) discontinuous viscosity solution of the adequate *nondegenerate* SFS equation when the mesh size vanishes.

7.4 Numerical algorithms for the generic SFS problem

For each scheme described in [40], we design (in [40]) an algorithm that computes some numerical approximations of a solution u^ρ of the considered scheme. Moreover, we prove that the computed numerical approximations converge toward u^ρ .

7.5 Examples of SFS results obtained from synthetic images

Let us recall that our method does not necessarily require boundary data. Figure 4 shows some reconstructions of the Mozart face when using the exact boundary data on the boundary of the image and at all critical points (Fig.4-c), when using the exact boundary data at all the critical points and state constraints on the boundary of the image (Fig.4-d), and with no boundary data, except for the tip of the nose (Fig.4-e). Let us remark that, as the theory predicted, our algorithms show an exceptional robustness to noise and errors on the parameters; This robustness is even bigger when we send the boundary to infinity (apply the state constraints). Figure 5 displays a reconstruction of Mozart’s face from an image perturbed by additive uniformly distributed white noise (SNR $\simeq 5$) by using the implicit algorithm (see [40]) with the wrong parameters $l_\varepsilon = (0.2, -0.1)$ and $f_\varepsilon = 10.5$ (focal length) and without any boundary data. The original image Fig.5-a) has been synthesized with $l = (0.1, -0.3)$ and $f = 3.5$. The angle between the initial light vector \mathbf{L} and the corrupted light vector \mathbf{L}_ε is around 13° .

¹⁶ equation associated with I_ε is *no more degenerate*.

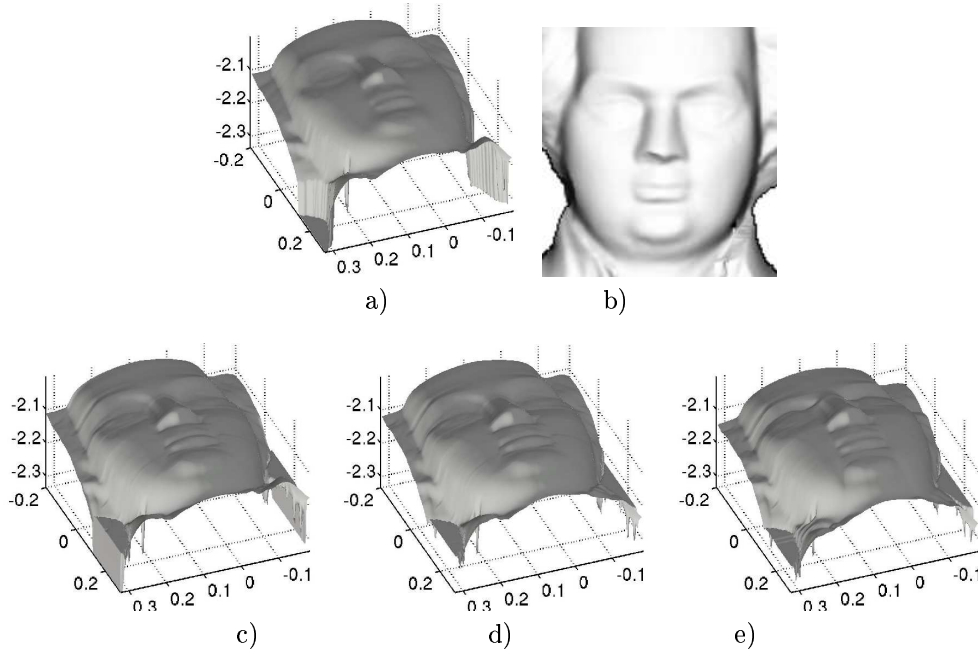


Figure 4: Reconstruction of Mozart's face *with and without* boundary data.

a) original surface; b) image generated from a) [size $\simeq 200 \times 200$]; c) reconstructed surface from b) with the implicit algorithm (IA) after only 3 iterations, using the exact boundary data on the boundary of the image and at all critical points: $\varepsilon_1 \simeq 0.56$, $\varepsilon_2 \simeq 0.0018$, $\varepsilon_\infty \simeq 0.42$; d) reconstructed surface by the IA (after 3 iterations) with state constraints on the boundary of the image: $\varepsilon_1 \simeq 0.58$, $\varepsilon_2 \simeq 0.0019$, $\varepsilon_\infty \simeq 0.42$; e) reconstructed surface by the IA (after 3 iterations) with state constraints on the boundary of the image and at all the critical points except at the one on the nose: $\varepsilon_1 \simeq 0.60$, $\varepsilon_2 \simeq 0.0020$, $\varepsilon_\infty \simeq 0.42$.

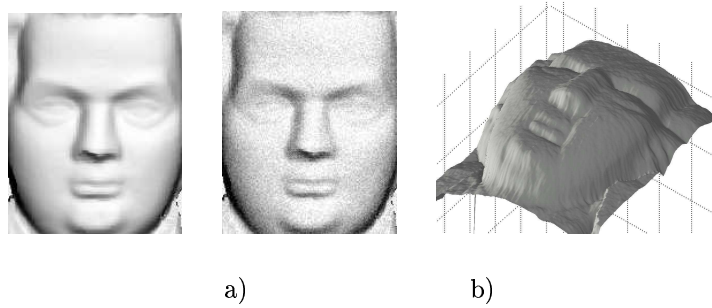


Figure 5: Reconstruction of Mozart's face from a noisy image with the wrong parameters $\mathbf{l}_\varepsilon = (0.2, -0.1)$ and $f_\varepsilon = 10.5$.

a) Image generated from Mozart's face represented in Fig.4-a) with $\mathbf{l} = (0.1, -0.3)$ and $f = 3.5$ [size $\simeq 200 \times 200$]; b) noisy image (SNR $\simeq 5$); c) reconstructed surface from b) after 4 iterations of the implicit algorithm, using the incorrect parameters $\mathbf{l}_\varepsilon = (0.2, -0.1)$ and $f_\varepsilon = 10.5$, and with state constraints on the boundary of the image and at all the critical points except at the critical point on the nose.

8 Toward applications of Shape from Shading

In this section, we suggest some *applications* of our SFS method. We do not provide complete descriptions, but we hope that the results will convince the reader of the *applicability of our SFS method to real problems*. Let us emphasize that all the results we present in this section are obtained from real images:

Note: When we apply SFS methods to real images we assume that the camera is geometrically and photometrically calibrated. In our experiments of sections 8.1 and 8.2 we know the focal length (5.8 mm) and approximately the pixel size (0.0045 mm; CCD size = 1/2.7") of our cheap digital camera (Pentax Optio 330GS). In section 8.3, we choose some arbitrary reasonable parameters. Also, note that there exist classical methods to calibrate photometrically a camera [33, 34]. In our tests, we do not use them, but we make some educated guesses for gamma correction (when the photometric properties of the images seem incorrect).

8.1 Document restoration using SFS

In this section, we propose a *reprographic system*¹⁷ to remove the geometric and photometric distortions generated by the classical photocopy of a bulky book. A first solution has been proposed by Wada and coworkers [53] who deal with *scanner* images involving a complex optical system (with a moving light). Here, the acquisition process we use is a classical camera¹⁸. The book is illuminated by a single light source located at infinity or close to the optical center (following the models we describe in section 2). Note that Cho et al. [15] propose a similar system but they use two light sources¹⁹. The acquired images are then processed using our SFS method to obtain the shape of the photographed page. Let us emphasize that, for obtaining a compact experimental system, the camera must be located relatively close to the book. Therefore the *perspective model is especially relevant* for this application. Also, the distortion due to the perspective clearly appears in the image a) of figure 8.

In our SFS method we assume that the albedo is constant. In this application, this does not hold because of the printed parts. Before recovering the surface of the page, we therefore localize the printed parts by using image statistic (similar to Cho's [15])²⁰ and we erase them automatically by using e.g. the inpainting algorithm of Tschumperle and Deriche [52]. This step can produce an important pixel noise. Nevertheless, this is not a problem for us because, as figure 7-b) shows, *our SFS method is extremely robust to pixel noise*: figure 7-b) displays the result produced by our algorithm (after 10 iterations) using the image of a text page with its pigmented parts, Fig.7-a). In this test, characters are considered as noise. Note that one could say that such a restoration system (based on SFS) is flawed because it does not use the information provided by the *rows* of characters. This is partially true but nevertheless, for pages containing few rows of characters but a lot of graphics and pictures (separated by large white bands²¹), such a SFS method could provide a simple and efficient solutions. Once we have recovered the three-dimensional shape of the page, we can flatten the surface by using e.g. the algorithm of Brown and Seales²² [8]. Note that at each step of this restoration process (3D reconstruction and flattening) we keep the correspondences with the pixels in the image. Thus, at the final step, we can restore the printed parts.

To prove the applicability of this method, we have tested it on a page mapped on a cylindric surface²³ (we have used our cheap camera and flash in an approximately dark room). Figure 8 shows the original image in a), the reconstructed surface (after 10 iterations) (textured by the ink parts of a)) in b) and an orthographic projection of the reconstructed surface, in c). Figure 8-c) indicates that our method allows to remove the perspective and photometric distortions.

8.2 Face reconstruction from SFS

The interest of the SFS methods for some applications dealing with faces has been demonstrated in e.g. the work of Zhao and Chellappa [57] (who use symmetric SFS for illumination-insensitive face recognition), by Smith

¹⁷Suggested to us by Durou (private communication); see [18].

¹⁸Note that a camera snapshot is practically instantaneous, whereas a scan takes several seconds.

¹⁹We can also note that the numerical method proposed by [15] requires that global variations of depth only exist along one direction. Our method does not require this hypothesis.

²⁰Most probably, we can also achieve this step by using the excellent work of Bell and Freeman [7] who propose a learning-based approach.

²¹This is often the case for scientific documents.

²²Not yet implemented, because of time.

²³For emphasizing the perspective effect.

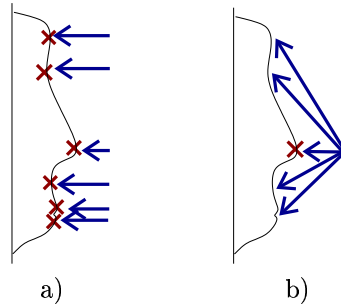


Figure 6: Critical points of the profile of a face. a) Critical points (6) for a homogeneous horizontal light; b) Critical point for a point light source at the optical center.

and Hancock [46] (who use SFS needle map for face recognition), and by Choi and coworkers [16] (who use SFS for determining the face pose). In this section we propose a very simple protocol based on SFS for face reconstruction. We use one camera equipped with a basic flash in an approximately dark place. As shown in figure 6, the interest of this method lies in the fact that, with such a protocol, the generated image should contain a unique critical point (if the distance of the face to the camera and the focal length are sufficiently small). Therefore, the propagation of the height information starts from this unique critical point.

We have tested our generic algorithm on a real image of a face²⁴ located at $\simeq 700$ mm of the camera in an approximately dark place (see Fig.9-a)). Figure 9-b) shows the surfaces recovered by our generic algorithm (after 5 iterations) with the perspective SFS model with a point light source at the optical center. As in the previous application, the albedo is not constant over the whole image. Therefore we removed the eyes and the eyebrows in the image by using e.g. the inpainting algorithm of Tschumperle and Deriche [52]. Moreover, note that this step can be automated by matching the image²⁵ to a model image already segmented. Figure 9 shows in c) the surface recovered from the image obtained after the inpainting process.

8.3 Potential applications to medical images

In this section, we are interested in applying our SFS method to some medical images. Our interest is motivated by the work of Craine et al. [19], Okatani and Deguchi [35], Forster and Tozzi [25], Smithwick and Seibel [47], Yeung et al. [55], Gillies et al. [50, 30] and Yamany et al. [54]. For illustrating the relevance of the “perspective SFS” modeling with the light source located at infinity, we apply our algorithm to an endoscopic image of a normal stomach²⁶ (see figure 10-a)). In fact, for producing such an image, the light source must be very close to the camera, because of space constraints. In figure 10-b), we show the result obtained (after 3 iterations) by our generic algorithm in the perspective case with the light source at the optical center. In figure 10-b), the surface is visualized with a light source located at the optical center. This reconstruction looks quite good. To further show the quality of the reconstruction, we display in c), the surface b) with a different illumination. Finally, notice that the stomach wall is not perfectly Lambertian (see Fig.10-a)). This suggests the robustness of our SFS method to departures from the Lambertian hypothesis.

9 Conclusion

We have developed a new mathematical framework which **unifies various SFS theories** (in particular, it unifies the work of Lions et al. [32, 45], of Dupuis and Oliensis [20], of Falcone et al. [10, 22, 23] and of Prados and Faugeras [43, 41]) and **generalizes them to all SFS Hamiltonians**, (in particular, we generalize them to “perspective SFS” with a light source located at the infinity or at the optical center). The mathematical tools we design allow to:

- suggest some numerical methods and algorithms;
- certify the convergence of the algorithms, to guarantee their robustness and to describe their limitations;

²⁴Slightly made-up to be more Lambertian.

²⁵We can use for example the very robust multi-modal and non-rigid matching method proposed by Hermosillo and Faugeras in [26].

²⁶Suggested by Tankus and Sochen (private communication) and downloaded from <http://www.gastrolab.net/>.

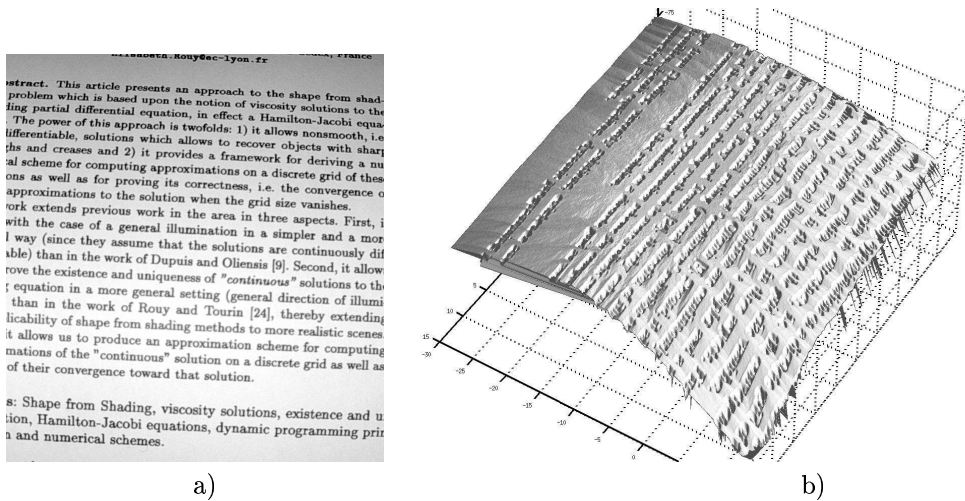


Figure 7: a) Real image of a page of text [size $\simeq 800 \times 800$]; b) Surface recovered from a) by our generic algorithm (without removing the printed parts of a)).

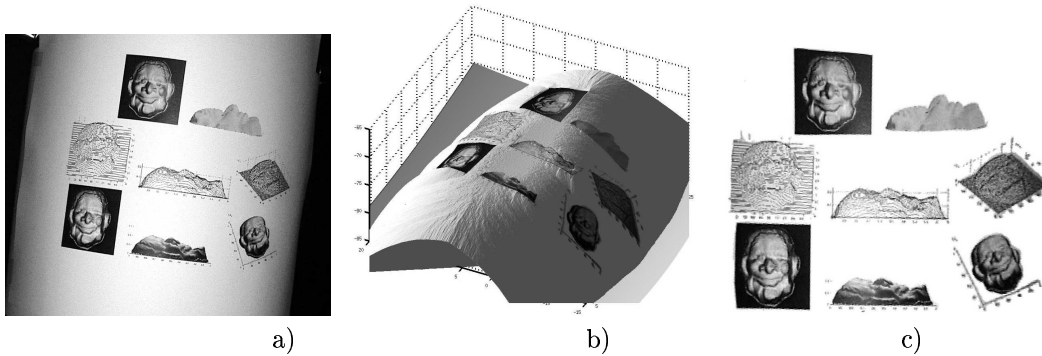


Figure 8: a) real image of a page containing pictures and graphics [size $\simeq 2000 \times 1500$], b) surface (textured by the printed parts of a)) recovered from a) by our generic algorithm (after having removed and inpainted the ink parts of a)). c) An orthographic projection of the surface b): the geometric (and photometric) distortions are significantly reduced.

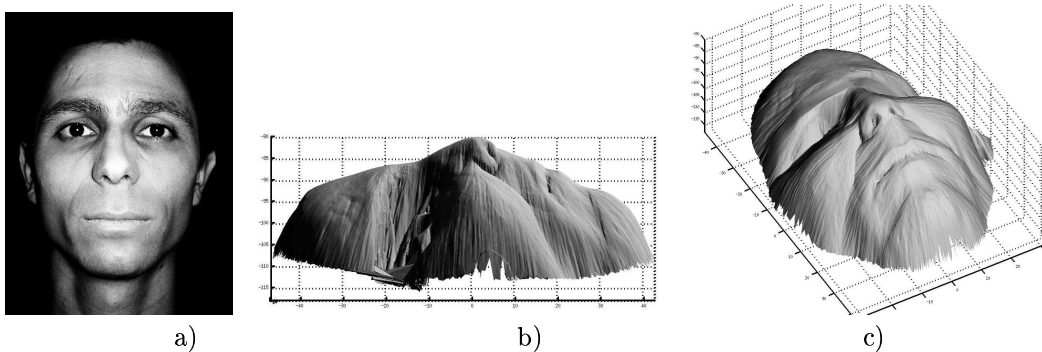


Figure 9: Face reconstruction from SFS: a) Real face image [size $\simeq 450 \times 600$]; b) surface recovered from a) by our generic algorithm with the perspective model with the light source located at the optical center; c) surface recovered by our generic algorithm with the same modeling hypotheses after the inpainting process.

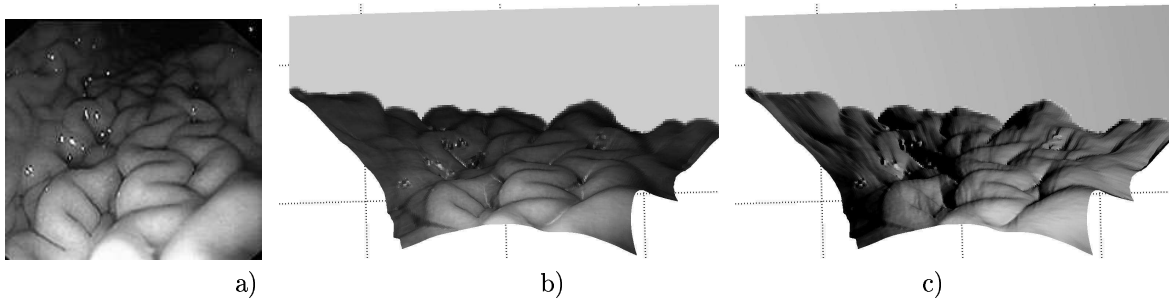


Figure 10: Reconstruction of a normal stomach: a) Original image of a normal stomach [size $\simeq 200 \times 200$]; b) surface recovered from a) by our generic algorithm with the perspective model and with the light source located at the optical center; c) surface b) visualized with a different illumination.

- better understand what we compute. In particular, when the problem has several solutions, it allows to characterize all the solutions, a necessary preliminary step for deciding which solution we want to compute.

The class of weak solutions we have defined in this paper is really more adapted to the SFS specifications than the other classical notions used in [32, 45, 10, 22, 23, 43, 41]; in particular, it **does not necessarily require boundary data**.

We have successfully applied our SFS method to **real images** and we have suggested that it may be useful in a number of **real-life applications**. We are extending our approach to non Lambertian SFS and to SFS with discontinuous images.

References

- [1] M. Bardi and I. Capuzzo-Dolcetta. *Optimal control and viscosity solutions of Hamilton-Jacobi-Bellman equations*. Birkhauser, 1997.
- [2] G. Barles. An approach of deterministic control problems with unbounded data. *Ann. Ist. Henri Poincaré*, 7(4):235–258, 1990.
- [3] G. Barles. *Solutions de Viscosité des Equations de Hamilton–Jacobi*. Springer–Verlag, 1994.
- [4] G. Barles and B. Perthame. Comparison principle for dirichlet-type hamilton-jacobi equations and singular perturbations of degenerated elliptic equations. *Applied Mathematics and Optimization*, 21:21–44, 1990.
- [5] G. Barles and P.E. Souganidis. Convergence of approximation schemes for fully nonlinear second order equations. *Asymptotic Analysis*, 4:271–283, 1991.
- [6] I. Barnes and K. Zhang. Instability of the eikonal equation and shape from shading. *ESAIM: Mathematical Modelling and Numerical Analysis (M2AN)*, 34(1):127–138, 2000.
- [7] M. Bell and W.T. Freeman. Learning local evidence for shading and reflectance. In *Proceedings of the International Conference on Computer Vision (ICCV)*, volume 1, pages 670–677, Vancouver, Canada, July 2001. IEEE Computer Society, IEEE Computer Society Press.
- [8] M. S. Brown and W. B. Seales. Document restoration using 3D shape. In *Proceedings of ICCV’01*, July 2001.
- [9] F. Camilli. *A characterization of the value function for a class of degenerate control problems*, volume 59 of *Series on advances in mathematics for applied sciences*, chapter 3, pages 47–58. World Scientific, 2001.
- [10] F. Camilli and M. Falcone. An approximation scheme for the maximal solution of the shape-from-shading model. *International Conference on Image Processing*, pages 49–52, 1996.
- [11] F. Camilli and A. Siconolfi. Maximal subsolutions for a class of degenerate hamilton-jacobi problems. *Indiana Univ. Math. J.*, 48(3):1111–1132, 1999.
- [12] F. Camilli and A. Siconolfi. Nonconvex degenerate Hamilton-Jacobi equations. *Mathematische Zeitschrift*, 242:1–21, 2002.
- [13] F. Camilli and A. Siconolfi. Hamilton-jacobi equations with measurable dependence on the state variable. *Adv. Differential Equations*, 8(6):733–768, June 2003.
- [14] I. Capuzzo-Dolcetta and P.-L. Lions. Hamilton-jacobi equations with state constraints. *Trans. Amer. Math. Soc.*, 318(2):643–68, 1990.
- [15] S.I. Cho and H. Saito. A Divide-and-Conquer Strategy in Shape from Shading problem. In *Proceedings of CVRP’97*, June 1997.
- [16] K.N. Choi, P. Worthington, and E.R. Hancock. Facial pose using shape-from-shading. In *Proceedings of BMVC’99*, pages 402–411, 1999.
- [17] F. H. Clarke. *Optimization and Nonsmooth Analysis*. SIAM, Classics in Applied Mathematics 5, 1990.
- [18] F. Courteille, A. Crouzil, J.-D. Durou, and P. Gurdjos. Shape from Shading en conditions réalistes d’acquisition photographique. In *Proceedings of RFIA’04*, 2004.
- [19] B.L. Craine, Craine E.R., C.J. O’Toole, and Q. Ji. Digital imaging colposcopy: Corrected area measurements using Shape-from-Shading. *IEEE Transactions on Medical Imaging*, 17(6):1003–1010, December 1998.
- [20] P. Dupuis and J. Oliensis. An optimal control formulation and related numerical methods for a problem in shape reconstruction. *The Annals of Applied Probability*, 4(2):287–346, 1994.
- [21] J.-D. Durou and H. Maître. On convergence in the methods of Strat and Smith for shape from shading. *The International Journal of Computer Vision*, 17(3):273–289, 1996.

- [22] M. Falcone and M. Sagona. An algorithm for the global solution of the shape-from-shading model. *International Conference on Image Analysis and Processing*, 1:596–603, 1997. LNCS 1310.
- [23] M. Falcone, M. Sagona, and A. Seghini. A scheme for the shape-from-shading model with "black shadows". In *Proceedings of ENUMATH 2001*, 2001.
- [24] P. Favaro, A. Mennucci, and S. Soatto. Observing shape from defocused images. *The International Journal of Computer Vision*, 52(1):25–43, April 2003.
- [25] C.H.Q. Forster and C.L. Tozzi. Towards 3d reconstruction of endoscope images using shape from shading. In *13th Brazilian Symposium on Computer Graphics and Image Processing (SIBGRAPI)*. IEEE Computer Society, October 2000.
- [26] G. Hermosillo and O. Faugeras. Dense image matching with global and local statistical criteria: a variational approach. In *Proceedings of CVPR'01*, 2001.
- [27] B.K. Horn and M.J. Brooks, editors. *Shape from Shading*. The MIT Press, 1989.
- [28] H. Ishii and M. Ramaswamy. Uniqueness results for a class of Hamilton-Jacobi equations with singular coefficients. *Comm. Par. Diff. Eq.*, 20:2187–2213, 1995.
- [29] J. Kain and D.N. Ostrov. Numerical shape-from-shading for discontinuous photographic images. *The International Journal of Computer Vision*, 44(3):163–173, 2001.
- [30] C.K. Kwoh, G.N. Khan, and D.F. Gillies. Automated endoscope navigation and advisory system from medical imaging. In *Proceedings of SPIE'99*, volume 3660, 1999.
- [31] P.-L. Lions. *Generalized Solutions of Hamilton-Jacobi Equations*. Number 69 in Research Notes in Mathematics. Pitman Advanced Publishing Program, 1982.
- [32] P.-L. Lions, E. Rouy, and A. Tourin. Shape-from-shading, viscosity solutions and edges. *Numer. Math.*, 64:323–353, 1993.
- [33] C.S. McCamy, H. Marcus, and J.G. Davidson. A colorrendition chart. *J. App. Photog. Eng.*, 2:95–99, 1976.
- [34] G.W. Meyer. Wavelength selection for synthetic image generation. *Computer Vision, Graphics, and Image Processing*, 41:57–79, 1988.
- [35] T. Okatani and K. Deguchi. Shape reconstruction from an endoscope image by shape from shading technique for a point light source at the projection center. *Computer Vision and Image Understanding*, 66(2):119–131, May 1997.
- [36] J. Oliensis. Uniqueness in shape from shading. *The International Journal of Computer Vision*, 2(6):75–104, 1991.
- [37] J. Oliensis and P. Dupuis. A global algorithm for shape from shading. In *Proceedings of ICCV'93*, pages 692–701, 1993.
- [38] D.N. Ostrov. Extending viscosity solutions to eikonal equations with discontinuous spatial dependence. *Nonlinear Anal.*, 42(4):709–736, 2000.
- [39] E. Prados and O. Faugeras. Une approche du "Shape from Shading" par solutions de viscosité. Master's thesis, Université de Nice Sophia-Antipolis, France, INRIA, September 2001.
- [40] E. Prados and O. Faugeras. A mathematical and algorithmic study of the lambertian SFS problem for orthographic and pinhole cameras. Technical Report RR-5005, INRIA, November 2003.
- [41] E. Prados and O. Faugeras. "Perspective Shape from Shading" and viscosity solutions. In *Proceedings of the 9th International Conference on Computer Vision*, volume 2, pages 826–831, Nice, France, October 2003. IEEE Computer Society, IEEE Computer Society Press.
- [42] E. Prados and O. Faugeras. A rigorous lambertian shape-from-shading method for orthographic and pinhole cameras. *Submitted to IJCV*, 2004.

- [43] E. Prados, O. Faugeras, and E. Rouy. Shape from shading and viscosity solutions. In A. Heyden, G. Sparr, M. Nielsen, and P. Johansen, editors, *Proceedings of the 7th European Conference on Computer Vision*, volume 2351, pages 790–804, Copenhagen, Denmark, May 2002. Springer-Verlag.
- [44] E. Prados, O. Faugeras, and E. Rouy. Shape from shading and viscosity solutions. Technical Report 4638, INRIA, November 2002.
- [45] E. Rouy and A. Tourin. A Viscosity Solutions Approach to Shape-from-Shading. *SIAM Journal of Numerical Analysis*, 29(3):867–884, June 1992.
- [46] W.A.P. Smith and E.R. Hancock. Face recognition using Shape-from-Shading. In *Proceedings of British Machine Vision Conference (BMVC)*, pages 597–606, September 2002.
- [47] Q.Y.L. Smithwick and E.J. Seibel. Depth enhancement using a scanning fiber optical endoscope. In *Proceedings of SPIE BiOS*, 2002.
- [48] H. M. Soner. Optimal control with state space constraints. *SIAM J. Contr. Optim*, 24:Part I: 552–562, Part II: 1110–1122, 1986.
- [49] P. Soravia. Optimal control with discontinuous running cost: eikonal equation and shape from shading. In *39th IEEE Conference on Decision and Control*, pages 79–84, December 2000.
- [50] L. E. Sucar, D. F. Gillies, and H. Rashid. Integrating shape from shading in a gradient histogram and its application to endoscope navigation. In *Proceedings of 5th International Conference on Artificial Intelligence (ICAI-V)*, 1992.
- [51] D. Tschumperlé. *PDE's Based Regularization of Multivalued Images and Applications*. PhD thesis, Université de Nice-Sophia Antipolis, December 2002.
- [52] D. Tschumperlé and R. Deriche. Vector-valued image regularization with PDE's : A common framework for different applications. In *IEEE Conference on Computer Vision and Pattern Recognition*, Madison, Wisconsin (United States), June 2003.
- [53] T. Wada, H. Ukida, and T. Matsuyama. Shape from shading with interreflections under proximal light source-3D shape reconstruction of unfolded book surface from a scanner image. In *Proceedings of ICCV'95*, June 1995.
- [54] S.M. Yamany and A.A. Farag. A system for human jaw modeling using intra-oral images. In *IEEE-EMBS*, volume 20, pages 563–566, 1998.
- [55] S.Y. Yeung, H.T. Tsui, and A. Yim. Global shape from shading for an endoscope image. In Chris Taylor and Alan C. F. Colchester, editors, *Proceedings of Medical Image Computing and Computer-Assisted Intervention (MICCAI)*, volume 1679 of *Lecture Notes in Computer Science*, pages 318–327, September 1999.
- [56] R. Zhang, P.-S. Tsai, J.-E. Cryer, and M. Shah. Shape from Shading: A survey. *IEEE Transactions on Pattern Analysis and Machine Intelligence*, 21(8):690–706, August 1999.
- [57] W. Zhao and R. Chellappa. Illumination-insensitive face recognition using symmetric Shape-from-Shading. In *proceedings of CVPR'00*, pages 1286–1293, 2000.

List of Figures

1	Examples of continuous (versus discontinuous) viscosity solution of (1)	5
2	Solutions of Eikonal equation with nonsuitable kinks	5
3	solutions of H versus $-H$; minimal solutions	25
4	Reconstruction of Mozart's face without boundary data	27
5	Reconstruction of Mozart's face from a noisy image with the wrong parameters	27
6	Critical points of the profile of a face.	29
7	3D reconstruction of an inked page from a real image	30
8	Reduction of the geometric and photometric distortions	30
9	Face reconstruction from SFS	30
10	Reconstruction of a normal stomach	31

Contents

1	Introduction	3
2	Hamiltonians for the Lambertian SFS problem	3
2.1	"Orthographic SFS" with a point light source at infinity	3
2.2	"Perspective SFS" with a point light source at infinity	4
2.3	"Perspective SFS" with a point light located at the optical center	4
2.4	A generic Hamiltonian	4
3	Weaknesses of the previous theoretical approaches of the SFS problem	4
4	Singular discontinuous viscosity solutions with Dirichlet boundary conditions and state constraints (SDVS)	6
4.1	Singular viscosity supersolutions of (2)-(7)	8
4.1.1	The multivalued map	8
4.1.2	A new Hamiltonian with the same multivalued map	9
4.1.3	Adaptation of the topology	9
4.1.4	Definition of singular viscosity supersolutions and solutions	10
4.2	Existence of the singular solution of (2)-(7)	11
4.3	Uniqueness results	14
4.4	Stability of the singular solution	15
4.4.1	A general stability result	15
4.4.2	Applications of the stability to the Shape from Shading	17
5	A general framework for SFS	21
6	Minimal and global viscosity solutions	24
7	Numerical approximation of the SDVS for generic SFS	25
7.1	Management of the state constraints	25
7.2	Regularization of the generic SFS equation	26
7.3	Approximation schemes for the nondegenerate SFS equations	26
7.4	Numerical algorithms for the generic SFS problem	26
7.5	Examples of SFS results obtained from synthetic images	26
8	Toward applications of Shape from Shading	28
8.1	Document restoration using SFS	28
8.2	Face reconstruction from SFS	28
8.3	Potential applications to medical images	29
9	Conclusion	29



Unité de recherche INRIA Sophia Antipolis
2004, route des Lucioles - BP 93 - 06902 Sophia Antipolis Cedex (France)

Unité de recherche INRIA Futurs : Parc Club Orsay Université - ZAC des Vignes
4, rue Jacques Monod - 91893 ORSAY Cedex (France)

Unité de recherche INRIA Lorraine : LORIA, Technopôle de Nancy-Brabois - Campus scientifique
615, rue du Jardin Botanique - BP 101 - 54602 Villers-lès-Nancy Cedex (France)

Unité de recherche INRIA Rennes : IRISA, Campus universitaire de Beaulieu - 35042 Rennes Cedex (France)

Unité de recherche INRIA Rhône-Alpes : 655, avenue de l'Europe - 38334 Montbonnot Saint-Ismier (France)

Unité de recherche INRIA Rocquencourt : Domaine de Voluceau - Rocquencourt - BP 105 - 78153 Le Chesnay Cedex (France)

Éditeur
INRIA - Domaine de Voluceau - Rocquencourt, BP 105 - 78153 Le Chesnay Cedex (France)
<http://www.inria.fr>
ISSN 0249-6399